Chapter 4

Cryogenic Tribology in High-Speed Bearings and Shaft Seals of Rocket Turbopumps

Masataka Nosaka and Takahisa Kato

Additional information is available at the end of the chapter

http://dx.doi.org/10.5772/55733

1. Introduction

In recent years, as a rule, improvement of the reliability of liquid propellant rockets becomes an international technical problem for built-up of safe space transport systems. The high performance, liquid propellant rocket engines require high-pressured turbopumps to deliver extremely low temperature propellants of liquid oxygen (LO_2, boiling point 90 K) and liquid hydrogen (LH_2, boiling point 20 K) to a combustion chamber in engine [1]. In LO_2/LH_2 turbopumps, cryogenic high-speed bearings and rotating-shaft seals are very important parts to sustain high reliability of the high-rotating-shaft systems. The turbopump bearings are directly equipped in cryogenic propellants in pump side [2]. The shaft seal systems are also set up between the cryogenic pumps and the hot turbines to restrain the leakage of cryogenic propellants and hot turbine gas [3].

These bearing and shaft seals have to operate under poor lubricating conditions due to extremely small viscosity at cryogenic temperatures. Furthermore, the turbopump bearings and shaft seals have to overcome a severe high-speed operation that has several critical speeds demonstrating self-induced severe vibration of the rotating shaft. In order to develop turbopump bearings and shaft seals, many inexperienced technical and tribological problems must be solved for extremely low temperature and high speed of operational conditions. Such cryogenic tribological technology has been playing a key role in cryogenic turbopumps to achieve high reliability.

This chapter presents a topical review of cryogenic tribological studies (for about 30 years in Japan) on the research and development of the cryogenic high-speed bearings and shaft seals of rocket turbopumps [4, 5]. The high-speed bearings and shaft seals were continually studied for the LE-5 engine used in the Japanese H-I rocket (developed in 1986) and the LE-7 engine used in the H-II rocket (developed in 1994). The bearings and shaft seals used in LO_2/LH_2

turbopumps of the LE-5 and LE-7 had a rotational speed level of 50,000 rpm and had been studied and developed from the mid-1970 to the mid-1990. Specially, the all-steel bearings (made of AISI 440C) of the LH_2 turbopump of the LE-7 demonstrated high performance with high reliability at high-speed level at 2 million DN (40 mm x 50,000 rpm). The shaft seal systems in the LE-5/LE-7 turbopumps that used a mechanical seal, a floating ring seal (annular seal) and a segmented seal are also reviewed.

Furthermore, for future space transport systems to reduce launch cost and to increase efficiency, advanced rocket engines which are characterized by high durability (long life) and high performance (light weight) are required in recent years. Advanced bearing and shaft seal that have high durability, i.e., a long life of 7.5 hours for the turbopump bearings used in reusable space shuttle main engine (the SSME). Its required life is 15 times longer than that (30 minutes) of the turbopump bearings used in the LE-7. At the first time, the SSME turbopump bearings experienced a serious wear problem in LO_2 due to poor self-lubrication of the retainer [6]. In order to extend bearing life, the hybrid ceramic bearing with Si_3N_4 balls was used to reduce serious wear in the conventional all-steel bearing. A new type of the retainer having PTFE/bronze-powder insert was also developed to obtain sufficient self-lubrication of the hybrid ceramic bearing. Consequently, the improvement of the SSME turbopump bearings needed a long time of about 20 years [7].

Today, ultra-high speed level above 100,000 rpm is required to make a small and light turbopump for advanced second-stage engine. These advanced research and development are actively underway. In Japan, a new type of hybrid ceramic bearing having Si_3N_4 balls with a single guided retainer demonstrated excellent performance at an ultra-high speed of 120,000 rpm (3 million DN) in LH_2 and recorded the world's top speed (in 2001) [8]. The result of this bearing was applied to the LH_2 turbopump (rotational speed, 90,000 rpm) of the RL60 demonstrator engine (in 2003). The RL60 demonstrator engine was developed in the USA with international collaboration (USA, Japan, Russia and Sweden) and the LH_2 turbopump was developed by a Japanese company [9]. In Europe, for the VINCI engine under development, high-DN hybrid ceramic bearing was tested in LH_2 at a speed of 70,000 rpm (2.8 million DN) and continuous studies on a high-DN bearing was conducted at DN up to 3.3 million (120,000 rpm) in LH_2 (in 2005) [10]. Furthermore, in Russia, for the developed RD0146 engine, its rotational speed of the main LH_2 turbopump was 123,000 rpm (3.08 million DN), but detail of its bearing was unknown (in 2003) [11].

This chapter also reviews advanced bearings and shaft seals which were studied from the mid-1990 to the mid-2000 after the development of turbopump bearings and shaft seals of the LE-7 [4,5]. It is typical that a long-life bearing with single-guided retainer demonstrated a long operation for 12 hours under 50,000 rpm. A hybrid ceramic bearing having single-guided retainer and Si_3N_4 balls was able to demonstrate ultra-high-speed performance at speeds up to 120,000 rpm and show excellent performance under 3 million DN. An annular seal made of an Ag plated steel ring also presented two-phase seal performance at speeds up to 120,000 rpm.

These historical reviews are intended to help the technical succession to next young generation who challenges research and development of the future space transportation system. These

http://dx.doi.org/10.5772/55733

reviews are based on previous studies carried out by Japan Aerospace Exploration Agency (JAXA) at Kakuda Space Center. All materials used in this chapter have been published by papers.

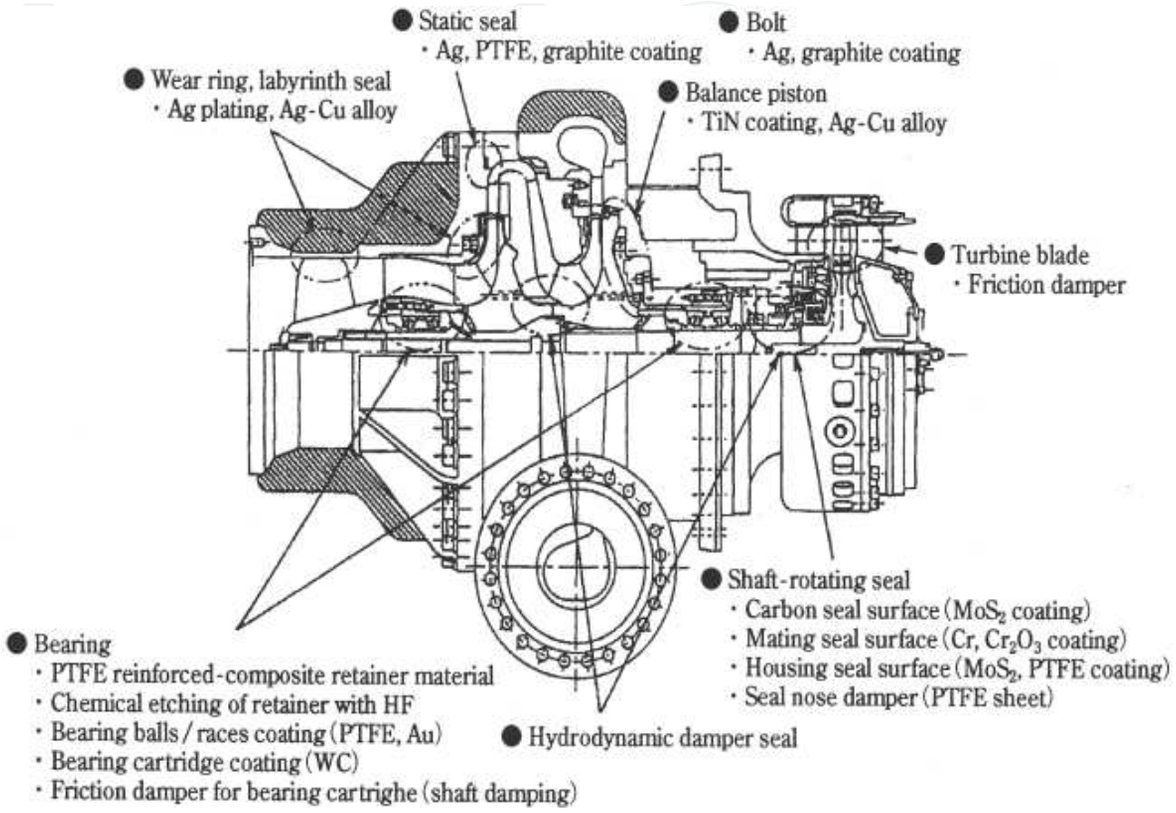

Figure 1. Typical tribo-components and solid lubricants used in turbopumps

2. Bearings and shaft seals of turbopumps

2.1. Turbopumps and tribo–components

The LO_2/LH_2 turbopumps as well as the tribo-components, such as high-speed bearings and rotating shaft-seals, were studied and developed to use in the LE-5 and LE-7. In reference to the structure of the LH_2 turbopump of the LE-7, the tribo-components and solid lubricants used in the LE-5 and LE-7 turbopumps are typically indicated in Fig. 1 [4]. In addition, main design parameters of the turbopumps and DN values of bearings for the LE-5 and LE-7 are listed in Table 1 [5]. Here, the DN value that represents high-speed level of bearing is defined as the product of the inner-race bore diameter D (in mm) and the pump rotational speed N (in rpm). The rotor speed is typically restricted by the DN limits of the bearing.

Engine (thrust)	LE-5 (10 tons)		LE-7 (86 tons)	
Rocket	Second stage of H-1		First stage of H-2	
Engine cycle	Gas-generator cycle		Staged-combustion cycle	
Turbopump	LO_2	LH_2	LO_2	LH_2
Pump pressure [MPa]	5.2	5.5	17.4 (25.8)*	27.0
Pump flow rate [kg/s]	20	3.6	212 (46)*	36
Shaft rotational speed [rpm]	16,500	50,000	18,000	42,000
Bearing DN [mm x rpm]	49.5×10^4	125×10^4	81×10^4	168×10^4
Turbine pressure [MPa]	0.48	2.4	19.1	20.6
Turbine temperature [K]	690	840	810	830
Turbine gas flow rate [kg/s]	0.39	0.42	14.9	33.6
Shaft power [kW]	130	490	4,700	19,700
Weight [kg]	23	25	160	200

For pre-burner in bracket; ( )*

Table 1. Design parameters of turbopumps and DN values of bearings for LE-5 and LE-7

a. *LE-5 turbopumps*

For the upper stage of the H-I rocket, the LE-5 had a gas-generator cycle with 10-ton thrust and its chamber pressure of 3.4 MPa was relatively low. Its engine cycle is not able to achieve a high engine performance due to an open cycle. For the LH_2 turbopump of the LE-5, the pump discharge pressure was relatively low at 5.5 MPa and the discharge flow rate was 51 liters/s. The turbine pressure was 2.4 MPa. The paired bearings of 25-mm bore operated at a speed of 50,000 rpm (1.25 million DN) and sustained the shaft power of 490 kW [12].

For the LO_2 turbopumps, the discharge pressure was 5.2 MPa and the discharge flow rate was 18 liters/s. The turbine pressure was 0.48 MPa. The paired bearings of 30-mm bore operated at a speed of 16,500 rpm and sustained the shaft power of 130 kW. Basic design and technology of the cryogenic tribo-components used in the small turbopumps was experimentally established under the development of the LE-5.

b. *LE-7 turbopumps*

For next technical challenge in the first stage engine of the H-II rocket, the LE-7 had a staged-combustion cycle (similar to that of the SSME) with 100-ton thrust and a high chamber pressure of 13 MPa. Its engine cycle can obtain high performance due to a closed engine cycle. For the high-pressure, large LH_2 turbopump of the LE-7, the pump discharge pressure was increased to 27 MPa, and the discharge LH_2 flow rate was 510 liters/s. The turbine pressure was relatively high at 20.6 MPa. The paired bearings of 35-mm bore were at the inducer side, and the paired bearings of 40-mm bore were at the turbine side. These bearings operated at a speed of 42,000 rpm (1.68 million DN) and sustained the shaft power of 19,700 kW [13,14].

For the LO_2 turbopumps, the discharge pressure was 18 MPa for the main pump and 26 MPa for the preburner pump, respectively. The total discharge LO_2 flow rate was 240 liters/s. The

http://dx.doi.org/10.5772/55733

turbine pressure was 19.1 MPa. The paired bearings of 32-mm bore were located at the inducer side and the paired bearings of 45-mm bore were at the turbine side. These bearings operated at a speed of 18,000 rpm and sustained the shaft power of 4,700 kW [14,15].

c. *Tribo-components in turbopumps*

As shown in Fig. 1, it is important to prohibit severe friction and wear in cryogenic environment that various solid lubricants are applied to the frictional parts in static and dynamic tribo-components. Since the turbopums are operated under large power conditions connecting with high fluid and mechanical vibration, it must pay attention that many components in contact are sure to generate relative motion and resulted in severe adhesive conditions. It needs proper lubrication to avoid severe frictional adhesion of assembled parts used in cryogenic environment.

The rotor of turbopump is directly supported by two sets of self-lubricated ball bearings in cryogenic pump fluid. The shaft seal of turbopump is installed between the cryogenic pump and the hot gas turbine. The shaft seal system must seal the cryogenic propellants and the combustion gases (steam with rich hydrogen gas) safely and securely. High-speed components, such as bearings, shaft seals, Labyrinth seals, wear rings and balance pistons, used the proper solid lubricants to protect them from severe friction and wear in the reduction (LH_2) or oxidation (LO_2) environment of the cryogenic propellants. It is noted that these high-speed tribo-components are important life-controlling parts in engines [4].

2.2. Self–lubricating bearings

2.2.1. Self–lubrication of retainer

The turbopump bearings are all-steel (AISI 440C) bearings that are self-lubricated by the PTFE transfer film as a lubricant from the reinforced PTFE (polytetra fluoroethylene) retainer. AISI 440C is martensitic stainless steel (with 16-18%Cr) and is one of the most widely used bearing materials in space systems because such high-Cr steel has a high corrosion resistance due to a superficial surface layer of Cr_2O_3. The resin PTFE retainer is reinforced with glass fiber, carbon fiber and laminated glass cloth to reduce wear as well as thermal contraction of the retainer. Although PTFE material has poor mechanical strength at room temperature, it has the best lubricant for use at cryogenic temperature because its mechanical tensile stress drastically increases and reaches to 80 MPa in LO_2 and 130 MPa in LH_2, respectively. In order to reduce wear of the PTFE composite retainer with poor thermal conductivity, sufficient cooling of the retainer is need to eliminate heat generation detrimental to successful bearing operation at high speeds [16].

Since LH_2 and LO_2 are particularly poor as lubricants because of their low viscosity under conditions of reduction or oxidation, hydrodynamic fluid lubrication is less effective. It is noted that the cryogenic pump fluids works to remove severe frictional heat and to prevent the temperature rise in the bearing. At low temperatures, the PTFE transfer film as a lubricant is kept to be hard and to sustain the bearing load, so that softening and rupturing of the transfer film due to a rise in temperature have to be eliminated. Under poor cooling conditions, it

appears that the blackened transfer film due to thermal decomposition of PTFE should occur at a high temperature above about 500 K, and the degraded transfer film was not able to sustain the bearing load. Therefore, sufficient cooling by cryogenic fluids, as well as reduction of frictional heat generation, is very important to produce a durable lubricant film transferred from the retainer even in cryogenic fluid [14].

2.2.2. High–speed and load conditions of bearing

For the turbopump bearings, angular-contact bearings are usually used in pairs in duplex mounts (back to back). For example, Table 2 shows main design parameters and internal load conditions for the bearings used in the LH_2 turbopumps of the LE-5 and LE-7 [17,18]. In this table, the *SVmax* value (=*Smax* x *Vmax*/2) that represents the maximum product of stress times spinning velocity in the contact ellipse zone at the inner race are shown. Here, *Smax* is the maximum contact stress and *Vmax* is the maximum spinning velocity. The *SVmax* value is an important factor related to lubrication and wear at the inner race with ball spinning [13,19]. High *SVmax* value leads to high frictional heating and to wear of the PTFE transfer film due to spin wear. Under poor cooling condition and large tilted misalignment, the turbopump bearings have an initial contact angel of 15-25 deg. with a large radial clearance to prevent a loss of operating clearance from bearing seizer. As mention later, high-speed bearing has the outer-race ball control that produces high ball spinning at the inner race. In order to reduce the stress level within the spinning contact zone, race curvatures were controlled to be 0.54-0.56 for inner race and 0.52 for the outer race, respectively. The inner race has a counter-bore type to gain sufficient cooling within the bearing.

As the centrifugal force developed on the balls increases at high speeds, the operational contact angle at the inner and the outer races are changed to be different each other. The operational contact angle at the inner race increases rather than the initial contact angle and decreases to near zero at the outer race. This divergence of contact angles tends to increase ball spinning in addition to rolling at the inner race. Its spin velocity due to ball spinning becomes high and results in an occurrence of frictional heat generation. To contrast, rolling contact at the outer race generates differential slip due to curvature of contact ellipse [20].

Under the outer-race control connected with ball spinning at the inner race, heat generation due to ball spin is significantly higher than that of differentia slip, so that sufficient cooling is necessary at the inner race side. Furthermore, sliding velocity of the rolling balls in contact with the outer guide land and the ball pocket is high and resulted in a generation of frictional heating of the retainer. The bearings were effectively cooled by the pump cryogenic fluids circulating in the turbopumps. For example, Fig. 2 shows sliding frictional conditions of the inner and outer raceways for the 25-mm-bore bearing that is at a speed of 50,000 rpm under a thrust load of 980 N [16]. This bearing was used in the LH_2 turbopump bearing for the LE-5. In this figure, the distribution of the contact stress, the spinning velocity and the *SV* value with spin at the inner race are shown. Pattern of spin wear generated by ball spinning becomes similar to the distribution of the *SV* value. To contrast, for the outer race, the differential slip velocity and the *SV* value with differential slip are light so that wear due to differential slip is

http://dx.doi.org/10.5772/55733

Parameters	LE-5	LE-7
Bearing		
Dimension [mm]	25 x 52 x 15	40 x 70 x 16
Pitch diameter [mm]	38.5	57
Ball diameter [mm]	7.938	9.525
Number of balls	11	13
Initial contact angle [deg.]	20	25
Initial radial clearance [μm]	57	137
Operating condition		
Rotational speed [rpm]	50,000	46,000
Thrust pre-load [N]	784	1,176
Bearing DN [mm x rpm]	125×10^4	184×10^4
Internal load condition		
Normal load at inner / outer races [N]	157 / 343	176 / 637
Maximum contact stress at inner / outer races (*Smax*) [GPa]	1.58 / 1.49	1.54 / 1.63
Maximum SV at inner race (*SVmax*) [N/mm^2 x m/s]	2.4×10^3	3.1×10^3

Table 2. Design parameters and internal load conditions for LH_2 turbopump bearings of LE-5 and LE-7

small. Furthermore, for the retainer, the sliding velocity is 50 m/s at the ball pocket and 45 m/s at the outer guide land at a speed of 50,000 rpm, respectively.

For system design of the turbopump high-speed rotor, the thrust load applied on the rotor due to unbalanced fluid pressures is balanced automatically by a balance piston mechanism during operation [17]. As a result, the turbopump bearings can operate only with a spring thrust load to remove internal clearance and control radial stiffness. However, the shaft vibration as well as the fluid action around the impeller should add high dynamic radial load to the thrust load on the bearing. For example, the LH_2 turbopump bearings of the LE-7 had to operate at a speed of 42,000 rpm that was beyond the third critical speed of 32,000 rpm and must support the high shaft-power under high shaft-vibration. Therefore, the bearings must have high combined radial and thrust load capacity at all extremes of the tutbopump operating conditions [14].

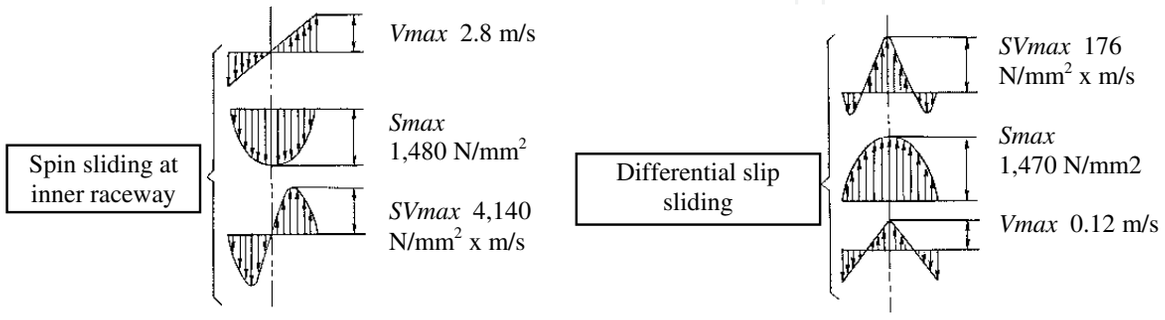

Figure 2. Sliding frictional conditions at inner and outer raceways for LH_2 bearing (25-mm bore, 50,000 rpm, 980 N)

2.3. Shaft seal systems

The required functions for shaft seal systems vary for different engine cycles. Similar to the SSME, the LE-7 has a two-stage combustion cycle. It requires a high pressure seal since the pressure in the pump and turbine is extremely high. To contrast, the pressure of the pump and turbine in the LE-5 with a gas generation cycle is comparatively low. Design parameters (the seal diameter, rubbing speed and seal pressure) for the seal elements used in the LE-5 and LE-7 turbopumps are listed in Table 3 [21]. The seal elements are the LO_2 seal, LH_2 seal, gas helium (GHe) purge seal and turbine gas seal. These shaft seals prevent or minimize the leakage of LO_2 and LH_2 for pump side and hot turbine gas (steam with rich hydrogen gas) for turbine side. In order to make a short length of the shaft, the shaft seals have to be compactly installed between the cryogenic pump and hot turbine.

Parameters	Seal diameter [mm]—Rubbing velocity [m/s] (Rotating speed [rpm])— Seal pressure [MPa]— Seal type	
Engine	LE-5	LE-7
LO_2 seal	46.6—40 (16,500)—0.98—(a)	55—58 (18,000)—4.9—(b)
LH_2 seal	43.2—113 (50,000)—1.4—(a)	50—120 (42,000)—7.1—(c)
GHe purge seal	40—35 (16,500)—0.3—(b)	69—173 (42,000)—0.6—(d)
Turbine gas seal	70—61 (16,500)—0.3—(b)	100—105 (18,000)—0.6—(b)
		55—58 (18,000)—16.7—(c)

(a) Mechanical seal, (b) Segmented seal, (c) Floating ring seal, (d) Lift-off seal

Table 3. Design parameters for seal elements used in LE-5 and LE-7 turbopumps

For the LO_2 turbopumps, when the leakage of LO_2 and hot turbine gas are mixed, an explosion will occur. In order to separate the leakage of LO_2 and hot turbine gas in safety, the system is complicated and requires three types of seal elements (the LO_2 seal, GHe purge seal and turbine gas seal). The GHe purge seal installed between the LO_2 seal and turbine gas seal supplies GHe as a barrier gas. To contrast, for the LH_2 turbopumps, the LH_2 leakage can be discharged to the turbine side so that the seal system is relatively simple. However, the rubbing speed of the seal face becomes considerably high and the contacting seal face is opposite severe tribological condition.

For the low-pressure turbopumps of the LE-5, the LO_2 and LH_2 seals used face-contact mechanical seals to gain small leakage. The GHe purge seal and turbine gas seal used contact-type segmented seal. For the high-pressure turbopumps of the LE-7, the LO_2 seal, LH_2 seal and turbine gas seal used non-contact type, floating-ring seal (annular seal) due to high seal pressure. For example, the shaft seal system of the high- pressure LO_2 turbopump of the LE-7 is shown in Fig. 3 [22]. The shaft seal system was set up between the cryogenic pumps and the hot turbine and prevented the mixing of the leakage of LO_2 and hot turbine gas. The LO_2 seal was composed of a floating-ring seal. The turbine gas seal used two floating-ring seals to seal the low temperature GH_2 that made a barrier to the turbine hot gas. So that the turbine gas seal

http://dx.doi.org/10.5772/55733

was kept at a lower temperature against the hot turbine section and the reliability of the shaft-seal system was further increased. Between the LO_2 seal and the turbine gas seal, the segmented circumferential seal (GHe purge seal), that had shrouded Rayleigh step hydrodynamic lift-pads to increase opening force, was paired and purged with GHe to prevent mixing of the leakage of LO_2 and GH_2.

The LH_2 seal system of the high pressured LH_2 turbopump was assembled with the floating-ring seal and lift-off seal. The lift-off seal is similar to a face-contact mechanical seal and is in contact with the mating ring (rotating seal-ring) and its leakage is small when the seal pressure is low. As the rotational speed of the turbopump increases and the seal pressure becomes high, the seal faces are automatically disengaged from contacting and changed to be non-contact seal [21].

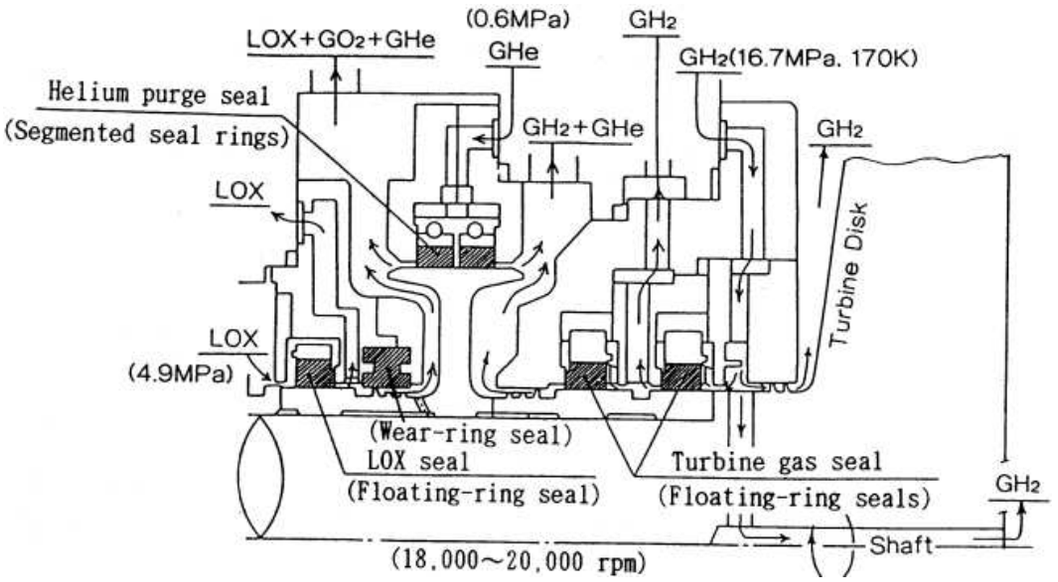

Figure 3. Shaft seal system for high-pressure LO_2 turbopump of LE-7

3. Cryogenic tribological problems [4, 16, 20, 23]

LH_2 is a particularly poor lubricant due to its extremely low viscosity (approximately equal to that of room-temperature air) and chemical reducing effect to remove native oxide film and to make fresh frictional surface, resulting in a severe lubricating condition at the frictional interfaces. Furthermore, at extremely low temperatures in LH_2, the specific heats and thermal conductivities of tribo-materials drop off rapidly rather than those at the liquid nitrogen (LN_2, boiling point 77 K) temperature. At a high temperature in LN_2, the specific heats and thermal conductivities are less changed and same as those at a room temperature. In addition with vaporization of LH_2, it is easy to produce local hot spots at frictional interfaces, so that frictional condition resulted in severe adhesive (welding) wear in LH_2.

LO_2 has high oxidization power and forms oxide film at frictional surfaces, so that oxide film produces lower friction compared with that in LH_2; however, in boiling of LO_2, oxide wear should increase due to high oxidization power. Active cooling is important to prohibit boiling of LO_2 at frictional interfaces. Furthermore, violent frictional heating in LO_2 can lead to the ignition of tribo-elements due to burn-out phenomenon occurring in nucleate boiling, that is defined by engineering heat transfer. Under burn-out phenomenon in boiling, an extreme rise in surface temperature was experienced because a marked reduction occurred in heat transfer. For example, in boiling of LN_2, the sliding surface of Ag-10%Cu alloy (melting point 1,155 K) against Ti alloy (Ti-5Al-2.5Sn) melted due to burn-out wear during friction test [24]. The surface coating of TiN or TiO_2 had a high resistance to adhesive welding to the Ti alloy disk was able to protect from burn-out wear. The results were applied to the balance-piston system in the LH_2 turbopump of the LE-7.

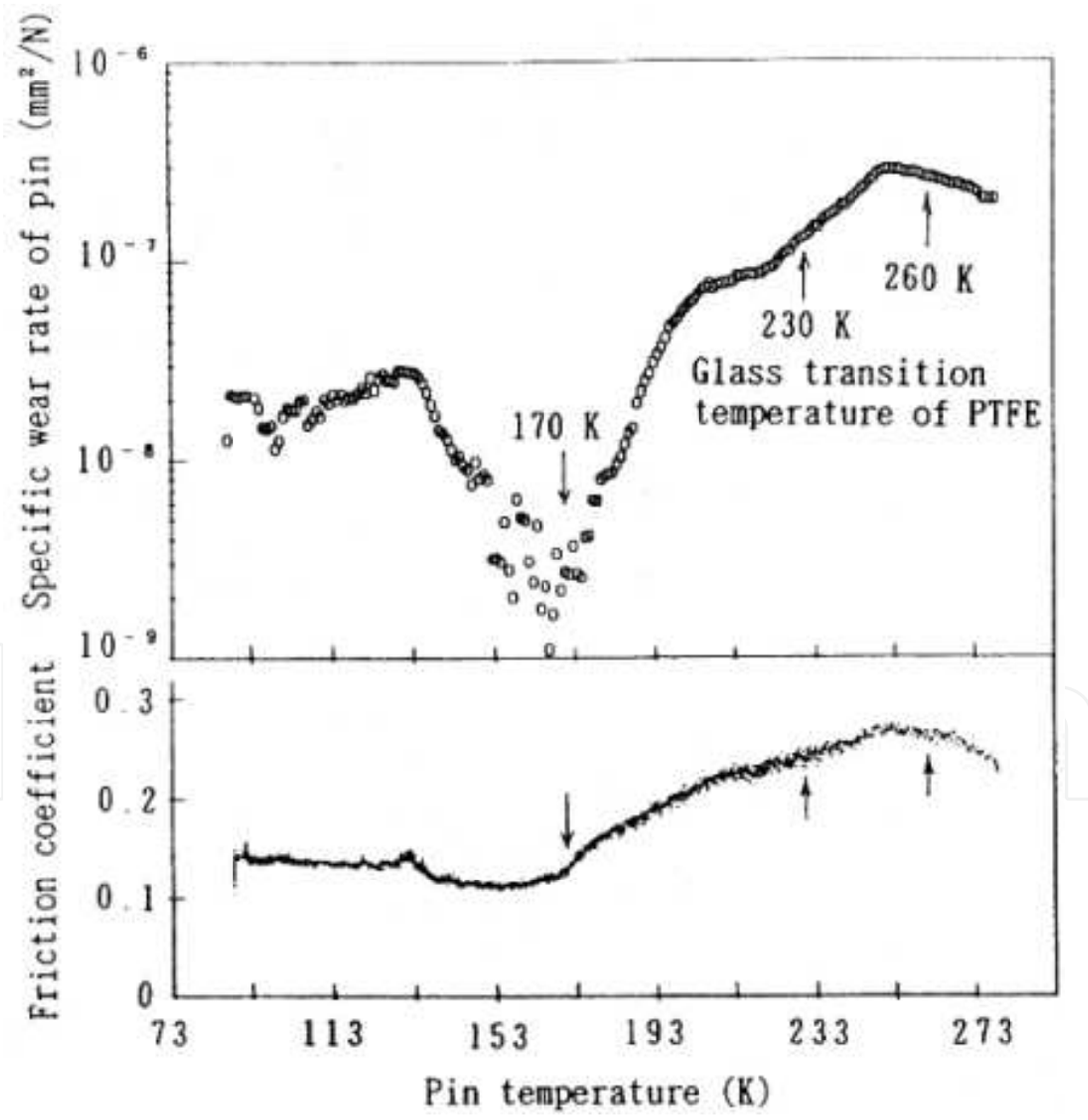

Figure 4. Friction and wear of PTFE pin against 440C disk in cryogenic GO_2 as a function of pin temperature

http://dx.doi.org/10.5772/55733

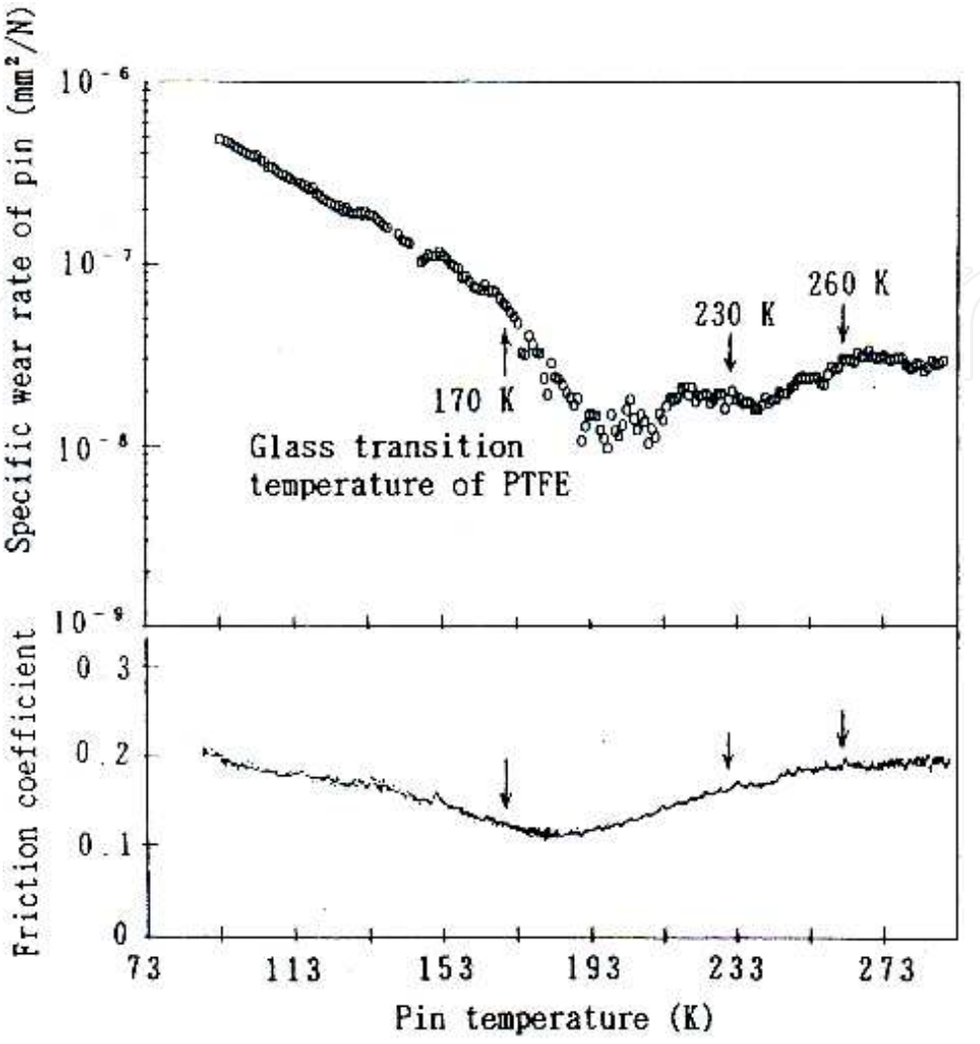

Figure 5. Friction and wear of PTFE pin against oxidized 440C disk in cryogenic GO_2 as a function of pin temperature

It is noted that the tribo-characteristics at cryogenic temperatures tend to change complexly. For example, Fig. 4 shows the change of friction and wear of a PTFE pin against a 440C steel disk in cryogenic gaseous oxygen (GO_2) as a function of pin temperature [23,25]. This figure denotes the glass transition temperature of PTFE, about 170 K, 230 K and 260 K, those are defined by relaxation of its amorphous layer in the PTFE band structure. When the frictional environment changed from the liquid phase to the gas phase at boiling, the friction coefficient increased drastically and wear began. To the glass transition temperature of 170 K (amorphous layer begins to relax), the friction coefficient remains at a low constant value, but the specific wear drastically decreased at 170 K. In an inert gaseous nitrogen (GN_2), there was not such drastically decrease in the specific wear at 170 K. After that, friction and wear begin to increase gradually up to 230 K. The increase of friction and wear above 170 K surely depends on the fact that the strength property of PTFE begins to decrease rapidly above 170 K.

However, when the surface of 440C steel was oxidized, the characteristic curve of friction and wear depended on cryogenic temperatures was changed drastically. Figure 5 shows the change

of friction and wear of a PTFE pin in case of using an oxidized 440C steel disk [23,25]. At the pin temperatures above boiling point of LO_2 (90 K), the friction and wear of PTFE pin showed relatively high values as compared with that showed in Fig. 4. As the pin temperature increased from 90 K to near 170 K, the friction and wear of PTFE drastically decreased to low values. The oxidized 440C steel disk was obtained by heating in air at about 623 K for 3 hours. The surface of the oxidized 440C showed an increase of FeO/Fe_2O_3 film in comparison with Cr_2O_3 film. It is noted that the oxidization of 440C steel should result in an increase of friction and wear of PTFE. It seems that PTFE transfer film was less formed due to poor adhesion of PTFE against FeO/Fe_2O_3, and frictional condition became to be severe. Thus, it is very interesting that the friction and wear properties of PTFE changed characteristically at its glass transition temperature, depending on the oxidization of 440C steel.

For other friction tests, wear of PTFE in cryogenic GO_2 was increased as surface roughness of 440C disk was increased; however, in cryogenic GN_2, surface roughness had less effect on wear increase of PTFE. Furthermore, friction and wear of PTFE against Si_3N_4 disk was determined in cryogenic GO_2 and GN_2. In both cryogenic environments, friction coefficient was higher than that of 440C disk. It was noted that wear of PTFE in GO_2 was drastically high compared with that in GN_2. It was assumed that poor formation of PTFE transfer film on the SI_3N_4 disk resulted in an increase of friction and wear in GO_2. This result indicated that the hybrid ceramic bearing with Si_3N_4 ball showed poor self-lubrication in LO_2.

It is interesting to use ceramic material as tribo-materials in cryogenic environments. Friction and wear behavior of typical fine ceramics against 440C disk were evaluated in LO_2 and LN_2. Figure 6 and 7 show wear and friction of five kinds of the ceramic balls in comparison with those in LO_2 and LN_2 [23], respectively. In all the cases of friction tests, the sliding contact surface of ceramic pin was covered by the transfer film of wear debris of 440C steel. The metallic transfer film prevented direct contact between metal and ceramic. As a result, the metal-to-metal contact should control the friction and wear behavior of the sliding pair, and the order of friction seemed to be less affected in the wear resistance of ceramic pins.

In LO_2, Al_2O_3 indicated the lowest wear rate and was followed by SiC, Si_3N_4, Sialon and ZrO_2 in order of the wear resistance. For Al_2O_3 pin, the metallic oxide film of 440C seemed to be strongly adhered onto the ceramic pin and resulted in an increase of protection of the pin wear; however, wear of the 440C disk was prolonged. For SiC, Si_3N_4 and Sialon, sliding friction in oxidized environment made the glassy formation of SiO_2 film due to tribo-chemical reaction. The hardness of SiO_2 is much less than that of ceramic substrate and resulted in an increase in the wear of ceramic pins. It was noted that the wear rate of ZrO_2 was considerably high as similar to that of self-mated 440C steels. Since ZrO_2 has the lowest hardness compared with other ceramics, the hard oxide film of 440C should increase wear of ZrO_2 pin.

To the contrary, in LN_2, Zr_2O_3 indicated the lowest wear rate and was followed by Si_3N_4, Sialon, Al_2O_3 and SiC in order of the wear resistance. The high wear of Al_2O_3 and SiC pins was seemed to be induced by lack of protective film of 440C steel due to weak adhesion to ceramic pin. It is found that the order of wear resistance of ceramics against 440C steel in LO_2 was opposed to that in LN_2 [23].

http://dx.doi.org/10.5772/55733

At cryogenic temperatures, it is noted that sufficient cooling and the restriction of frictional heat generation are essential to prohibit severe tribological conditions. In order to solve these cryogenic tribological problems, it is important that (1) understanding the complex characteristics of tribology at low temperatures, (2) selection of the proper solid-lubricants against the oxidation or reduction power, and (3) active cooling to remove severe frictional heat at local hot spots [4].

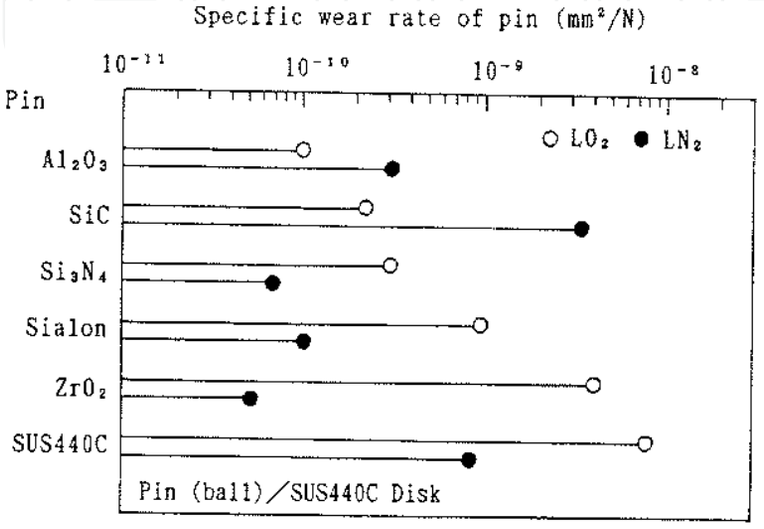

Figure 6. Wear of five kinds of the ceramic balls against 440C disk in LO_2 and LN_2

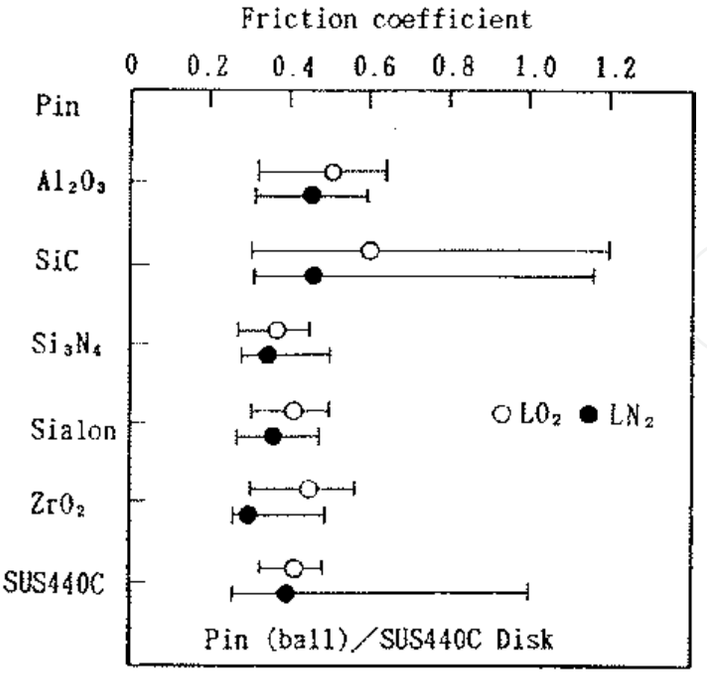

Figure 7. Friction of five kinds of the ceramic balls against 440C disk in LO_2 and LN_2

4. High–speed bearings

4.1. Improvement of self–lubrication of retainer [16, 17, 18, 26, 27]

In the beginning of the development of the turbopump bearing for the LE-5, the bearing had used the composite PTFE retainer reinforced with glass fiber or carbon fiber. The bearing tested in LH_2 by using a bearing tester showed that the glass fiber-reinforced PTFE retainer (24 wt.% glass fiber and additive) could demonstrate stable bearing-torque performance as compared with that of the carbon fiber-reinforced retainer (15 wt.% carbon fiber). From inspection of the ball-pocket surface of the carbon fiber-reinforced retainer, it was found that pile-up of the wear debris of carbon fiber might reduce supply of PTFE transfer film to ball surface. As a result, the LH_2 turbopump bearing selected the glass fiber-reinforced PTFE retainer; however, the real turbopump test showed severe wear of the retainer when the turbopump was operated under poor cooling conditions. This fact indicated low wear resistance of the glass fiber-reinforced PTFE retainer under severe operation of turbopump [16,17].

For the rocket-turbopump bearings, a laminated glass cloth with PTFE binder (laminated glass cloth of 45 wt.% and PTFE of 55 wt.%) was currently used because of its great strength to protect against dangerous retainer rupture [4,17]. This retainer showed poor self-lubrication resulting from abrasion by glass cloth layers exposed on the ball-pocket surface. During the development of the LH_2 turbopumps for the LE-5, the bearing showed unstable high-temperature rise and poor lubrication was observed, resulting in severe wear of the balls. In case of the reusable turbopumps used in the SSME, the bearings similarly experienced a serious wear problem [6]. In order to improve the self-lubricating performance of the retainer, special surface treatment of the retainer was developed [12,18]. The abrasive retainer surface with the exposed glass cloth was chemically etched with hydrofluoric acid (HF) to a depth of 0.10-0.15 mm. Following this treatment, smooth surface for the retainer was obtained. The sliding friction and wear between the ball and ball-pocket surface was reduced, resulting in a sufficient supply of PTFE transfer film from the retainer to the rolling balls.

For the HF etched retainer tested in LH_2, detailed examination of the transfer film on the sound ball surface with hardly any wear was conducted by electron probe microanalysis (EPMA) [12]. The result indicated that F of PTFE of the retainer strongly depended on the Ca concentration on the map and resulted in the tribo-chemical formation of CaF_2 transfer film. The reacted oxide material (49 wt.% of glass fiber) consisted mainly of an oxide of Ca (CaO) remained on the HF etched retainer surface. Therefore, it seems that the formation of CaF_2 transfer film was conducted by tribo-chemical reaction between F of PTFE and CaO remained on the retainer surface in chemical reduction environment in LH_2.

In order to determine the effect of tribo-chemical formation of CaF_2 in transfer film, additional friction tests were conducted. Figure 8 shows the wear of PTFE composite pins with 15 wt.% of various fillers against the 440C disk in cryogenic oxygen gas (GO_2, 123 K) under a high sliding speed (10 m/s) [15]. The PTFE composites with CaO and MgO fillers showed excellent wear resistance (progression of the pin-wear was stopped) due to the formation of good transfer film even in both cryogenic GO_2 and GN_2 (123 K). It seems that alkali-earth-metals

http://dx.doi.org/10.5772/55733

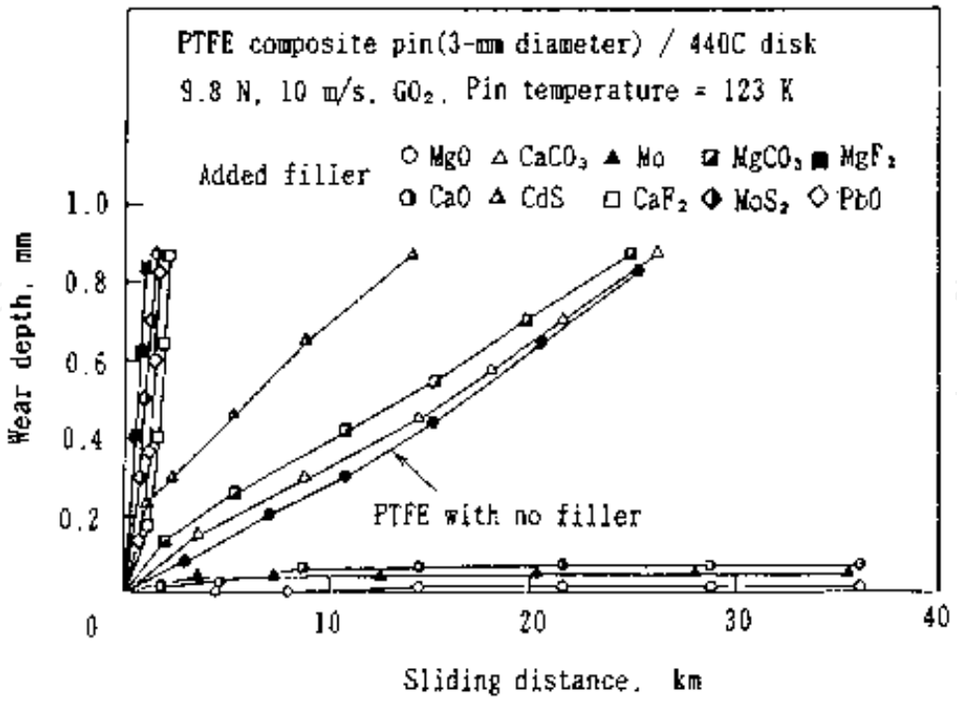

Figure 8. Wear of PTFE composite pins with various fillers against 440C disk in cryogenic GO_2 (123 K) under high-sliding speed (10 m/s)

such as Ca and Mg were able to react easily with F by severe dry sliding friction and resulted in the formation of CaF_2 and MgF_2 within the transfer film [4]. The tribo-chemical formation of CaF_2 and MgF_2 might enhance adhesion of transfer film. When CaF_2 and MgF_2 added as fillers to PTFE, there was no tribo-chemical reaction, resulting in poor wear resistance. Furthermore, oxidation of the Mo filler in GO_2 seemed to be extremely effective except in GN_2.

4.2. Development of elliptical ball–pockets of retainer [13, 14, 26]

During testing of the LH_2 turbopump for the LE-7, the conventional bearings using a retainer with circular pockets showed a significant temperature rise under high shaft vibration. Since high shaft vibration increases the radial load applied to the bearings, ball excursion occurring in the ball pockets of the retainer due to ball-speed-variation (BSV) becomes significantly large. Figure 9 shows the ball excursion due to the BSV *vs.* the radial load for the 40-mm-bore bearing at a speed of 42,000 rpm [13]. The ball excursion tends to increase with increasing of the radial load. At a radial load of about 1.5 times thrust load, the ball excursion reaches a maximum value. When the pocket clearance of the retainer is smaller than the maximum ball excursion, severe contact occurs between the ball and the retainer pocket.

For the 40-mm-bore bearing, a retainer having elliptical pockets with a large pocket clearance was developed. As shown in Fig. 10, this retainer with elliptical pockets is able to allow maximum ball excursion due to BSV in the circumferential direction and to stabilize wobbling of the retainer due to a narrow clearance in the axial direction [13]. The pocket clearance of 1.8 mm was twice as large as that of the conventional circular pocket. Consequently, the LE-7

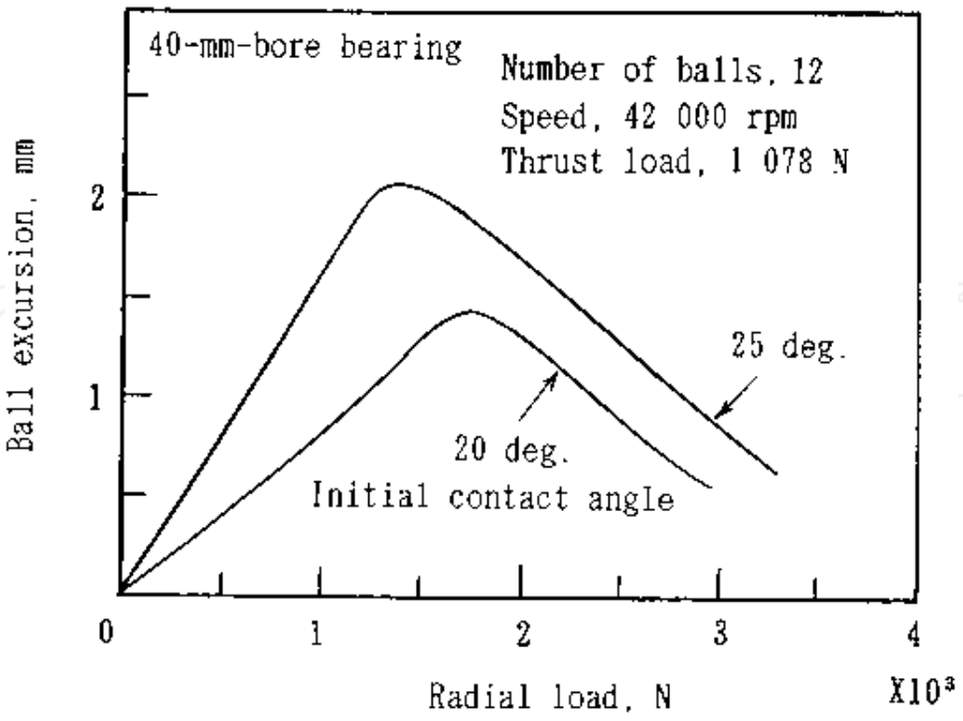

Figure 9. Ball excursion due to BSV *vs.* radial load for LE-7 LH_2 bearing at 42,000 rpm (40-mm-bore bearing)

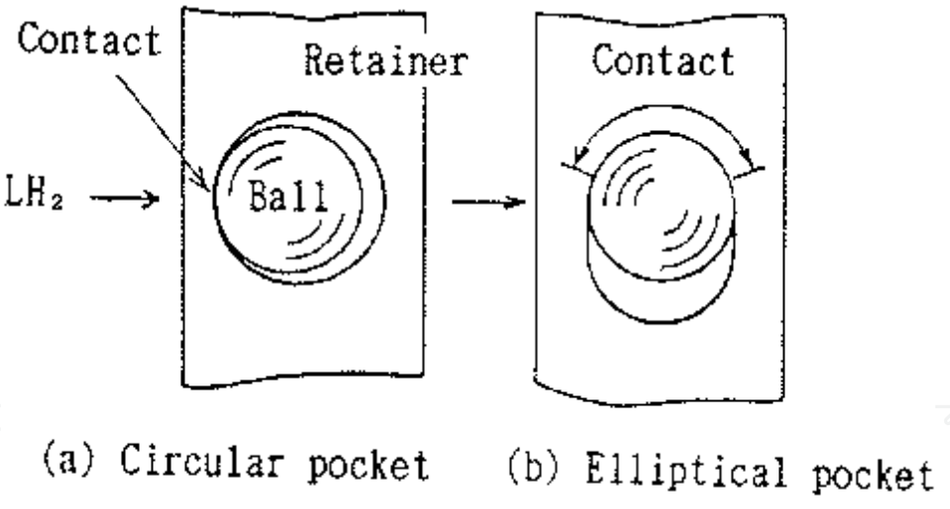

Ball pocket	Ball-pocket clearance, mm
Circular	0.9
Elliptical	1.8 (Circumferential)
	0.3 (Axial)

Figure 10. Circular and elliptical pockets of retainer and ball pocket clearances for 40-mm-bore bearing

http://dx.doi.org/10.5772/55733

turbopump bearings with the elliptical-pocket retainer exhibited excellent performance by reducing severe frictional heating and high wear of bearing components at a high-speed level of 50,000 rpm (2 million DN). Basic study of the elliptical pocket of the retainer was conducted in the development of the LE-5 turbopump bearing [12,17].

During the development of the LE-7A, the LH_2 turbopump experienced severe operation with high vibration of the rotating shaft. As a result, high vibration of the rotating heavy turbine-disk increased radial load at the turbine-side bearings (40-mm bore) and broke the retainer due to large BSV [26]. It was considered that the ball-retainer contact force due to BSV bent the retainer and hoop stress occurred on the retainer inside, resulting in fracture of the thin (weak) web section of the ball pocket. In order to gain high reliability of the LH_2 turbopump, the retainer using elliptical ball pocket was improved by increasing the pocket clearance to 2.2 mm.

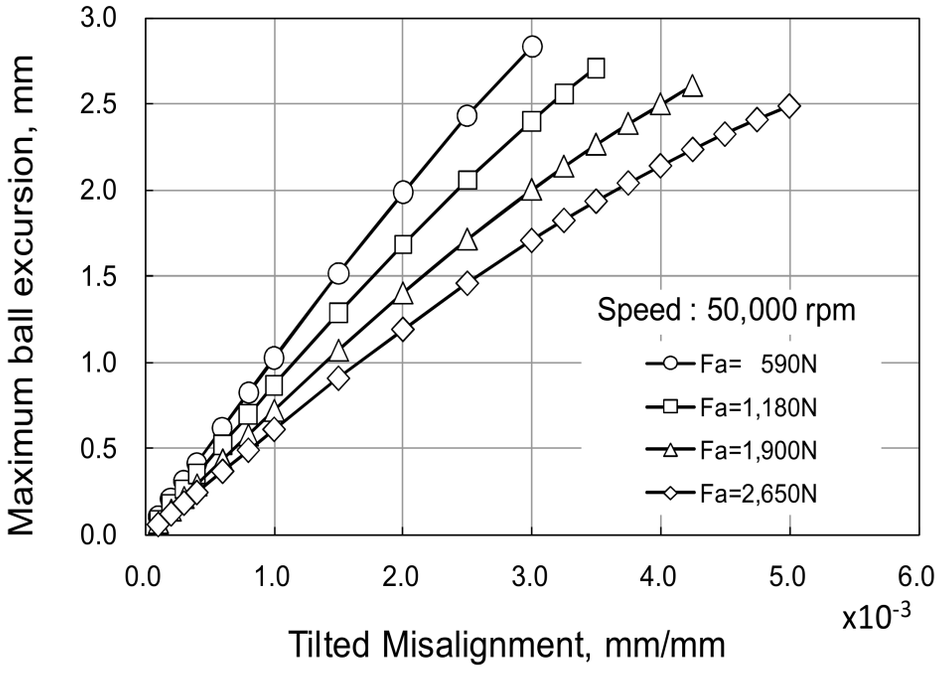

Figure 11. Maximum ball excursion vs. tilted misalignment under various thrust loads at 50,000 rpm (40-mm-bore bearing)

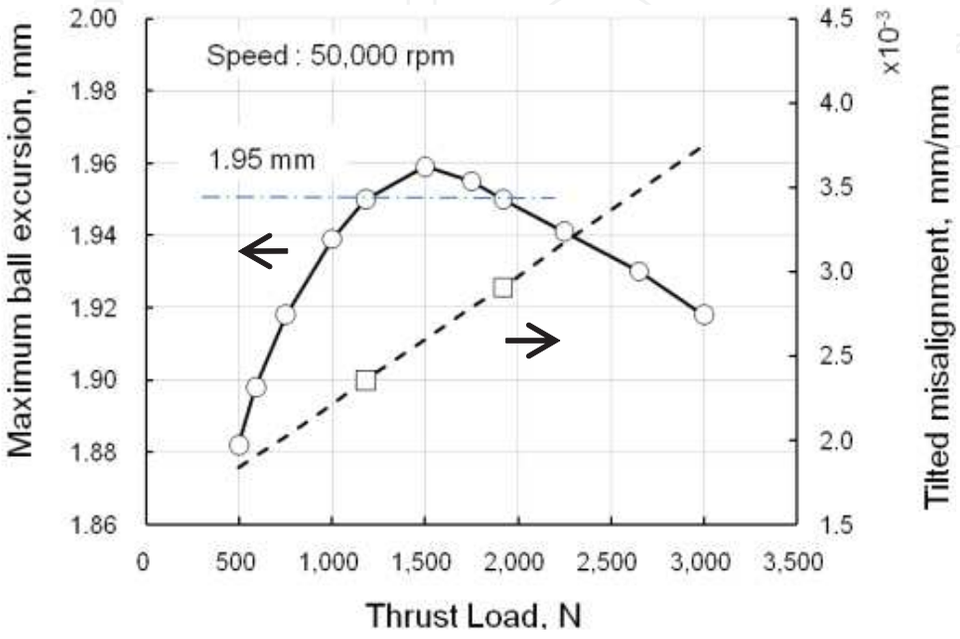

Figure 12. Maximum ball excursion and tilted misalignment *vs.* thrust load at 50,000 rpm (40-mm-bore bearing)

Such BSV was also caused by inclination of the outer race to the shaft (tilted misalignment). The effect of tilted misalignment in a level of 1.9-3.5 x 10^{-3} mm/mm on the tribo-characteristics of 40-mm-bore ball bearing was determined. The bearing used a retainer having various elliptical ball pockets to restrain the ball-retainer contact due to high BSV. The elliptical ball pocket changed the pocket clearance (1.75mm, 1.95 mm and 2.15 mm). Figure 11 shows the relationship of the tilted misalignment and the maximum ball excursion under various thrust loads at a speed of 50,000 rpm [26]. It is understood that maximum ball excursion increased with an enlargement of tilted misalignment.

Figure 12 shows the relationship of the maximum ball excursion and the tilted misalignment *vs.* the thrust load at a speed of 50,000 rpm [26]. The relationship of the maximum ball excursion *vs.* the thrust load was calculated by assuming that the tilted misalignment linearly increased with an increase of the thrust load. As the thrust load increased, the calculated maximum ball excursion tended to increase in a parabolic pattern. It was found that, in case of the pocket clearance of 1.95 mm, ball-retainer contact due to ball excursion possibly occurred within a limited range of thrust loads, resulting in high increase of bearing torque and bearing temperature.

http://dx.doi.org/10.5772/55733

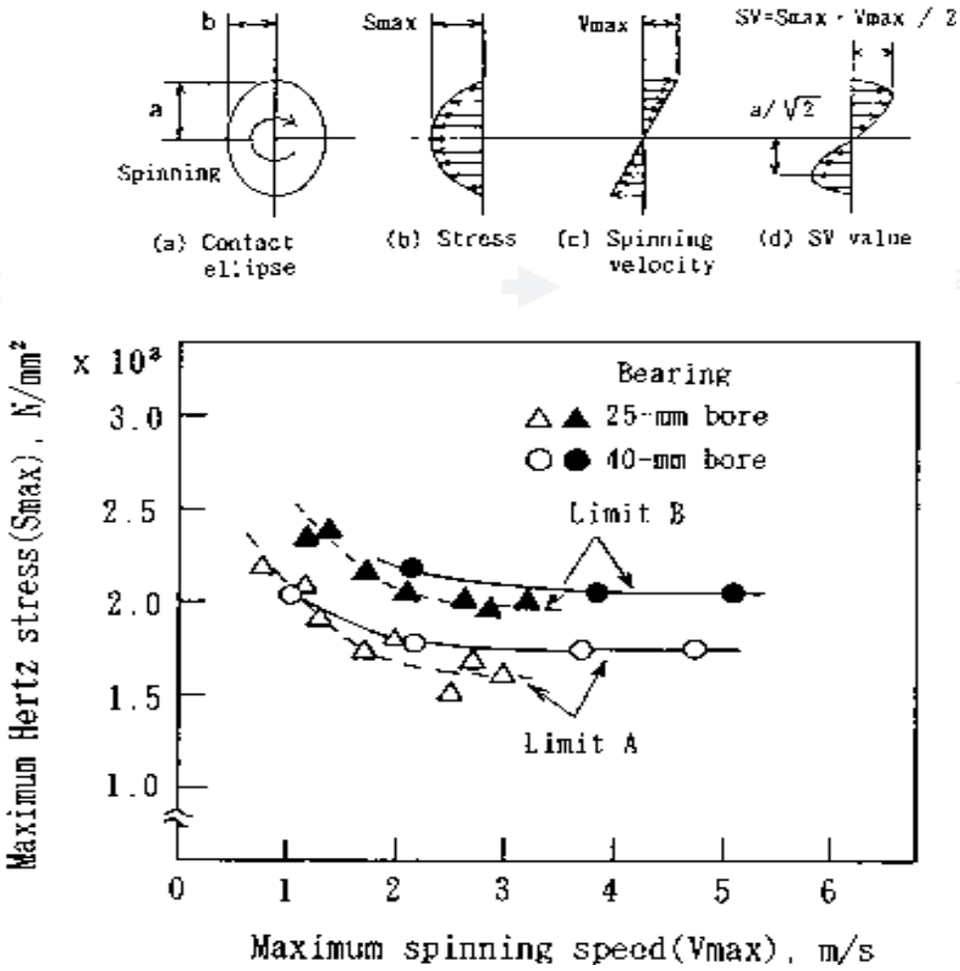

Figure 13. Load capacity of transfer film under inner race ball-spinning in LH_2

4.3. Performance of LH_2 bearing [12, 13]

Performance of self-lubricating bearing coated with PTFE or MoS_2 films was evaluated for the LH_2 turbopump bearing of the LE-5. The PTFE and MoS_2 films were coated with rf-sputtering. Bearing test was conducted for about 2 hours at a speed of 50,000 rpm in LH_2. Frictional heating was estimated from the temperature rise of cooling flow through the test bearing [12]. The coated films are hoped to induce smooth running in the initial operation when the amount of the PTFE transfer film is insufficient. The high self-lubricating performance and durability were experimentally confirmed with the PTFE coated bearing indicating frictional heating of 170-250 W. For the MoS_2 coated bearing, the frictional heating was 250-330 W and relatively high. The retainer of the PTFE coated bearing showed less ball-pocket wear than that of the MoS_2 coated bearing.

For high-speed bearings, since the bearing was under the outer-race ball control at high speed, the transfer film of the inner raceway was damaged due to the spinning of the ball. In order to evaluate stable operating condition without bearing damage, the load capacity of the transfer film under inner race ball-spinning in LH_2 was determined as shown in Fig. 13[13].

This figure shows the critical load capacity, that is, maximum Herze stress (*Smax*) *vs.* maximum spinning speed (*Vmax*). Under high thrust loads, an increasing of the bearing torque and bearing temperature (at limit A) was determined by the bearing tester which could measure the bearing torque in LH_2. The film local rupture (at limit B) was also defined by the electrical resistance monitoring between the inner race and outer race. Up to a *Vmax* of 5 m/s at 50,000 rpm, the transfer film was able to sustain a *Smax* up to 2 GPa. It was determined that the load capacity of the transfer film depended more on *Smax* than on *Vmax*. So, in order to increase durability of the bearing, it is important to limit the stress level to a *Smax* of 2 GPa to prevent transfer-film rupture and sufficiently to cool the frictional heat due to high *Vmax*.

4.4. Durability of LO_2 bearing [15]

It is noted that violent frictional heating in LO_2 can lead to the ignition of tribo-elements due to burn-out phenomenon. Burn out is overheat occurring in a transition from nucleate boiling to film boiling at critical heat flux that is defined by engineering heat transfer. For the LO_2 turbopump bearings (32-mm and 45-mm bore) of the LE-7, the durability and fatigue life were evaluated by applying heavy radial loads at a speed of 20,000 rpm in LO_2 or LN_2. During testing, the bearing-cartridge-acceleration (BCA), i.e., *Gpk* (peak value) and *Grms* (rot-mean-square value), was monitored to detect bearing damage. Testing in LO_2 for about 2.2 hours under a system radial load of 5,880 N showed that excellent lubricating conditions without abnormal BCA were obtained for all bearings.

Durability test in LN_2 (to keep safety in the experience) under a heavy system radial load of 11,760 N was conducted at a speed of 20,000 rpm for about 5.1 hours [15]. The result detected that the fatigue life of the bearing was about the same as the calculated B_{10} fatigue life. The bearings were operated at steady conditions for 5.1 hours with 20 start-stops. For BCA on bearings A/B, *Gpk* and *Grms* on the chart were abnormally separated from each other in a pattern of abnormal BCA showing an increase of surface roughness due to an occurrence of slight flaking. Then, at a total test time of 3.8 hours, the loaded and unloaded BCA abnormally began to increase concomitantly. Examination of tested bearing B indicted that slight flaking with very shallow depth (about 8.5 μm) was observed on the inner raceway.

4.5. Evaluation of turbopump bearings [14]

The durability of the bearings of the LO_2/LH_2 turbopumps used in the firing tests of the LE-7 was evaluated based of findings of wear inspection and X-ray photoelectron spectroscopic (XPS) analysis of PTFE transfer film. Inspection of the turbopump bearings used in the engine firing tests is essential for evaluation of their durability under engine operation.

a. *Bearing wear*

After the engine firing test, surface profiles of the raceways of the LH_2 turbopump bearings was evaluated [14]. The engine test was conducted for a total time of 31.4 minutes with 20 engine start-stops. The surface profiles included the thickness (1μm) of the initial film coatings of sputtered PTFE film. It is obvious that the wear scars on the raceways of all bearings were flat and spin wear was not observed despite conditions of higher ball spinning on the inner

http://dx.doi.org/10.5772/55733

raceway. For the retainer with elliptical pockets, the wear depths in the pockets were smaller than the depth (0.10-0.15 mm) of chemical etching of the glass cloth. The PTFE layer without the abrasive glass cloth sufficiently remained at the bottom of the pocket wear scar.

To contrary, the all inner raceways of the LO_2 turbopump bearings showed typical spin wear with light oxidative wear [14]. These turbopump bearings tested for a total time of 34.6 minutes with 23 engine start-stops. The surface profiles included the thickness of the initial film coatings of sputtered PTFE film (1 μm) on Ion-plated Au film (0.4 μm). The wear depths of raceways seemed to be relatively high; however, smooth surface roughness demonstrated mild wear without severe adhesion due to metal-to-metal. For bearing D that was affected by turbine whirling with radial overload, heavy spin wear with a wear depth of 7 μm was generated on the inner raceway. Furthermore, slight flaking was observed on the inner and outer raceways. This flaking was characterized by a very shallow depth and by fractures on the surface.

For the retainer with conventional circular pockets, the wear depths in the pockets were relatively light compared with those of the LH_2 bearing. The contact area in the retainer pocket and on the ball surfaces was blackened by the thermally degraded transfer film. The degradation of the transfer film seemed to occur at a temperature above about 500 K. This was confirmed by a heating test of the retainer. These facts indicated that the transfer film was severely heated even in cryogenic fluid and the LO_2 turbopump bearings were operated under poor cooling conditions. Thus, to increase the durability of the bearings, it is apparent that sufficient cooling is essential.

b. *XPS analysis of transfer films*

In order to evaluate the excellent lubricating conditions without severe wear, XPS depth analysis of a transfer film on a ball used in the LH_2 turbopump bearing of the LE-7 was conducted. Inspected ball that showed excellent wear condition was from the turbine-side bearing tested for 31.4 minutes in engine tests. The XPS depth analysis with an etching depth of 30 nm (SiO_2 rate) indicated that F(1s) and Fe(2p) spectra show the significant formation of thick CaF_2 and FeF_2 film as shown in Fig. 14 [4]. It seemed that, due to the reduction power of LH_2, the reacted CaO (remained on the retainer surface chemically etched with HF) was tribo-chemically changed to CaF_2 with the F of PTFE retainer during bearing operation. In addition, due to removing of native oxide film by the LH_2 reducing power, a FeF_2 film was formed by a chemical reaction between the F of PTFE retainer and the Fe of 440C steel. It is noted that the formation of FeF_2 film at the stressed contact area resulted in demonstrating high resistance to metal-to-metal adhesion and in leading to less wear [27].

Thus, the LH_2 turbopump bearings used in the engine firing tests demonstrated excellent performance due to the formation of thick CaF_2 and FeF_2 film. The tribo-chemical formation of CaF_2/FeF_2 film possibly reduced wear at frictional interfaces within the bearings used in LH_2. The basic tribo-chemical reaction was determined as follows [4]:

$$\left(\text{-}CF_2\text{-}\right)_n + CaO + Fe \rightarrow \left(\text{-}CF_2\text{-}CO\text{-}\right)_n + CaF_2 + FeF_2 \quad (1)$$

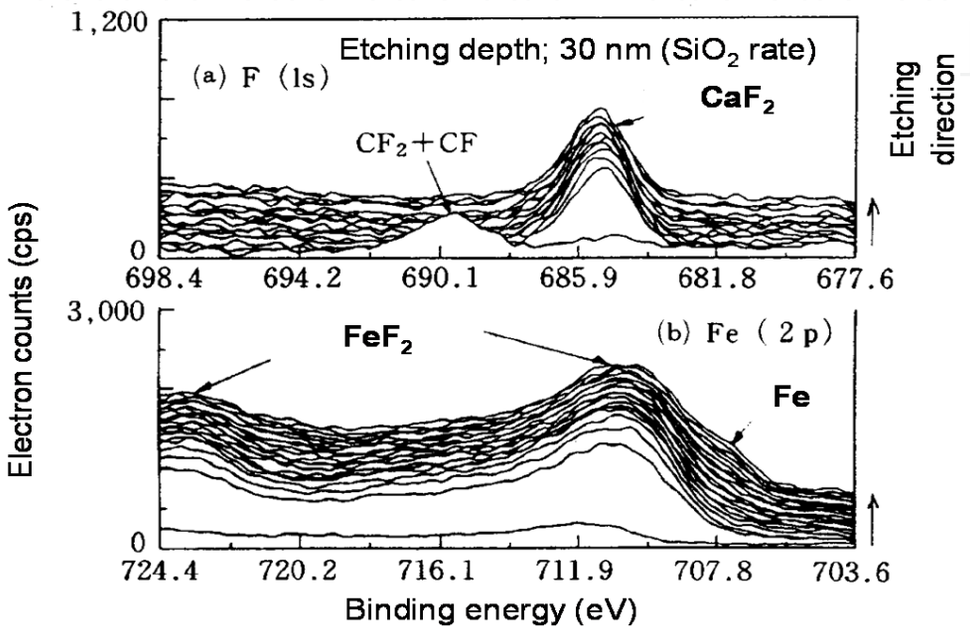

Figure 14. XPS depth analysis of ball for LH_2 turbopump bearing (turbine side)

On the contrary, for the LO_2 turbopump bearings of the LE-7, the inspected ball was from the turbine-side bearing that was tested for 34.6 minutes in engine tests and showed heavy spin wear. Figure 15 shows the XPS depth analysis with an etching depth of 30 nm (SiO_2 rate) for the worn ball due to spin wear. It indicated that the oxidization power of LO_2 prohibited the tribo-chemical formation of CaF_2 /FeF_2 transfer film. This bearing was operated under poor cooling conditions, so that the bearing wear was relatively increased and shallow flaking was formed on the raceways. From the F spectrum, it was shown that very thin PTFE/CaF_2 transfer film was formed compared with the thick PTFE/CaF_2 transfer film in the LH_2 bearing. Furthermore, from the Fe spectrum, formation of Fe_2O_3 oxide film was typically shown. Fe_2O_3 oxide film was apt to form at elevated temperature, so that the oxidative mild wear in the bearing was increased due to poor cooling conditions in LO_2 [5]. As mention later (in 6.1.1), for the bearing tested under sufficient cooling condition, the intense formation of Cr_2O_3 film without Fe_2O_3 film was found beneath an extremely thin PTFE film, resulting in high resistance to metal-to-metal adhesion and in a decrease of the bearing wear [28].

http://dx.doi.org/10.5772/55733

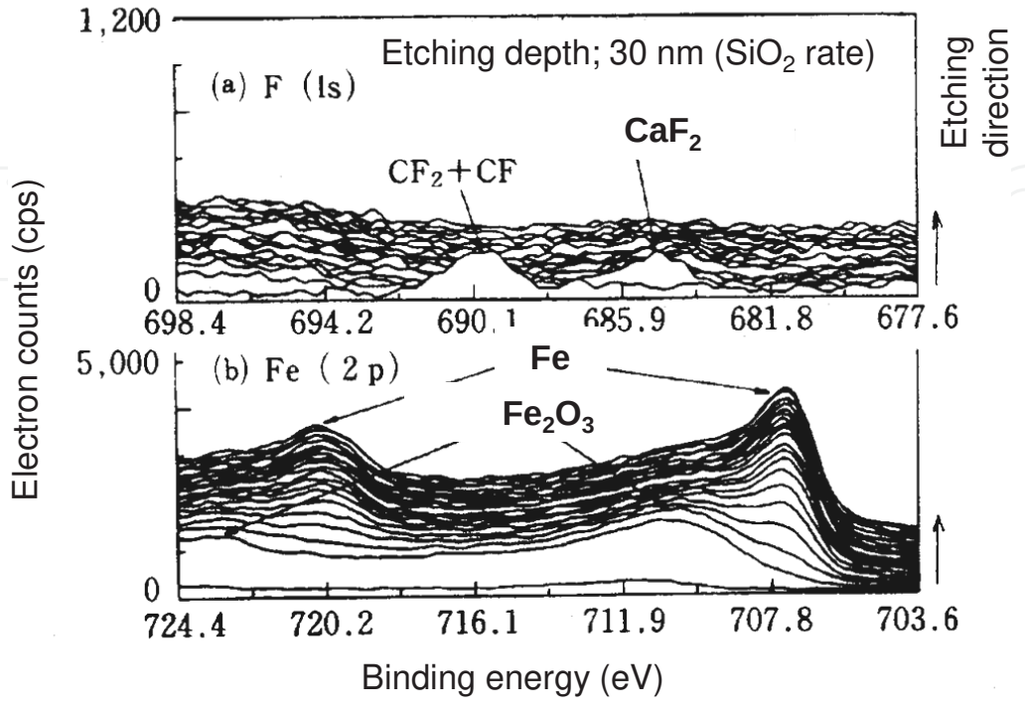

Figure 15. XPS depth analysis of ball for LO_2 turbopump bearing (turbine side)

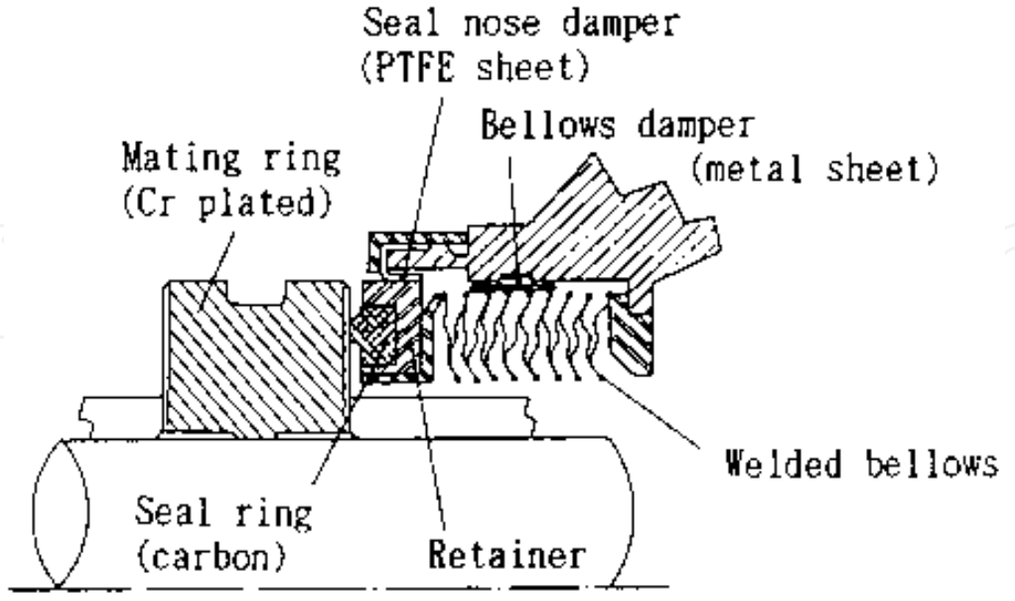

Figure 16. Face-contact mechanical seal for LH_2 turbopump of LE-5

5. Turbopump shaft seals

5.1. Mechanical seal [29-34]

For the LE-5 turbopumps operating under the gas generator cycle, the contact-type mechanical seal was able to use for the propellant seals because the pump and turbine pressures were relatively low. Specially, for the LH_2 turbopump, a high-speed mechanical seal was required to withstand high rubbing speed (113 m/s) at a speed of 50,000 rpm in LH_2. Figure 16 shows the face-contact mechanical seal with a seal diameter of 43.2 mm developed for the LH_2 turbopump of the LE-5 [29,30]. In order to reduce seal leakage of LH_2, it has a modified seal nose that could reduce the seal face distortion and control the direction of its distortion (to contact at outside of the seal face) under low temperature and high pressure. Furthermore, a modified vibration damper made of PTFE sheets is attached around the seal nose to prevent fluttering during rapid start or stop of the turbopump.

When the closing force to contact seal faces is increased to make seal leakage smaller, wear rate of the seal faces is increased due to the poor lubrication of LH_2. If the closing force is set to be smaller than the fluid opening force separating seal face each other, the leakage is considered to be quite large because of the extremely low viscosity and density of LH_2. Therefore, to obtain the stable seal performance and the long wear life, it is important that the proper balance between the closing force and the opening force is retained.

Critical value of the seal balance ratio that obtained stable seal performance and reduce wear of the seal faces was experimentally and analytically evaluated [32,33]. In this study, the experimental and analytical study on the friction power loss and seal performance was conducted. It was indicated that the friction power loss fell to a small value after the seal faces were sufficiently run-in. The seal balance ratio *[B]* that stabilized seal performance was in a range of 0.77-0.82. The seal balance ratio *[B]* is determined by the following equation;

$$\left[B\right] = B + Fsp / \left(As\Delta P\right) \tag{2}$$

where, B is the fluid balance ratio, Fsp is the spring force of bellows, As is the seal area and $\triangle P$ is the seal pressure. *[B]* is determined by the initial spring force of the bellows.

When the seal balance ratio was below 0.77, the leakage was apt to increase due to lack of the closing force. In this case, the critical balance ratio *[B]c* that gains stable seal performance showing small leakage was 0.77. To contrast, its balance ratio above 0.82 increased wear of the seal face by rise of the closing force. This high value of critical balance ratio was due to large opening force that could be explained with leakage flow model, assuming the phase change of leakage (from liquid phase to gas-liquid phase and gas phase) due to viscous frictional heating at high rubbing speed. In this phase change model, a state change of gas was assumed to be irreversibly adiabatic and a curve of gas expansion expressed by the following equation;

http://dx.doi.org/10.5772/55733

$$Pv^m = \text{constant} \tag{3}$$

where, P is the pressure, v is the specific volume and m is the ausfluss exponent. As m decreases with the temperature rise of gas due to viscous friction, the pressure of leakage flow increases particularly in the gas region within gas-liquid phase, and it resulted in the increase of the opening force. The analysis of phase change model of leakage was conducted using the flow and energy equations of liquid and gas leakages.

Figure 17 shows the calculated and experimental results of the relationship between the seal clearance and the opening force ratio *[K]* at a speed of 50,000 rpm in LH_2. The opening force ratio *[K]* is expressed by the following equation;

$$[K] = Fo / (As\Delta P) \tag{4}$$

where, *Fo* is the opening force. It was also shown that the opening force within seal clearance increases linearly as the seal clearance decreases. After the seal faces were sufficiently run-in and the seal clearance was maintained in an average of 0.6 μm, the opening force ratio *[K]* approaches the critical balance ratio *[B]c* (=0.77) that showed critical seal performance. As a result, the difference of *[K]* and *[B]c* was decreased and it resulted in the reduction of the load on the seal faces. The frictional loss power was decreased to a small value, resulting in a restrain of wear rate of seal faces. If the seal clearance increases, the leakage becomes large; however, the load on the seal faces is increased with the decrease of the opening force and the seal clearance would become small enough to reduce leakage. Furthermore, the starting torque and static seal performance were markedly affected by the change of the seal face distortion due to wear [31].

Durability of the mechanical seal was evaluated by the long-run test [29]. The long-run test was conducted at a speed of 50,000 rpm with a seal pressure of 1.37 MPaG for 83 minutes. The experimental results showed that the leakage gradually increased until total test time was 50 minutes. During its step, wear of the seal faces was running-in, then the leakage was stabilized. It is noted that an extremely small LH_2 leakage (8-19 cc/min) was kept during test. The seal after the durability test indicated an excellent condition that maximum wear of carbon-ring was 8 μm.

Temperature on the rubbing seal faces was estimated from the reduction rate of the hardness of hard Cr plating on the rotating mating ring [34]. The estimated temperature of rubbing seal face was possibly reached to be about 773 K at a rubbing speed of 113 m/s in LH_2. In an initial stage of running-in, extremely high temperature of the seal faces caused thermal cracks in wear surface of the Cr plating, so that it is necessary to cool the contacting seal faces sufficiently. When the cooling of the sealing unit is insufficient, the surface of the carbon seal ring showed abnormal wear. Furthermore, the Cr plating showed better wear results than the tungsten carbide (WC) coating, because the Cr plating easily forms thin transfer films of graphite contained in the carbon. In the case of the WC coating, the transfer film of graphite was hardly formed in LH_2, resulting in an occurrence of severe seal wear.

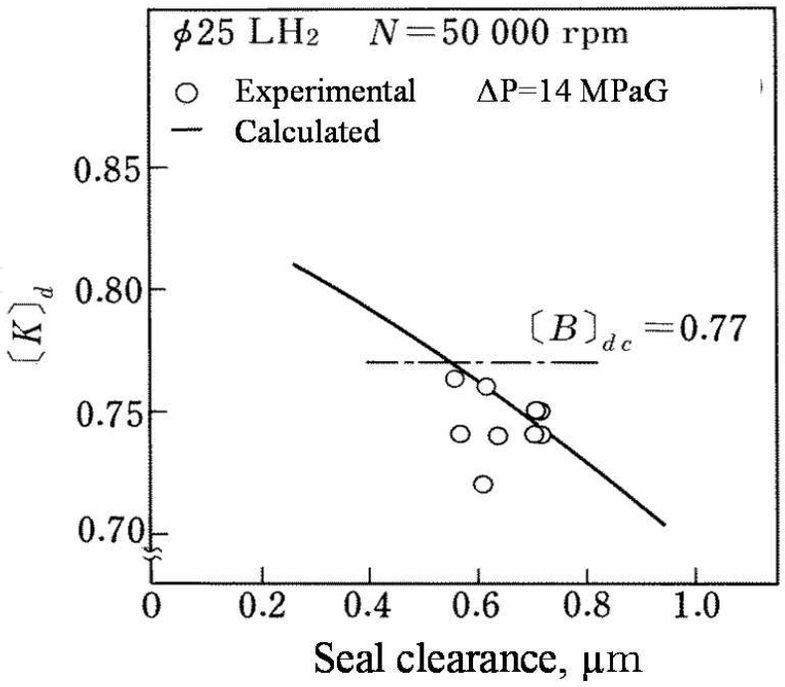

Figure 17. Opening force ratio *[K]vs.* seal clearance at 50,000 rpm in LH_2

5.2. Floating ring seal [22, 29, 35, 37]

A floating-ring seal is a type of no-contact annular seal without a rubbing seal surface. It has a simple structure and is able to seal high-pressure fluids, restraining leakage through a small clearance (gap) between the seal ring and the runner. Its gap is in an order of several dozens of μm. The seal ring is free to move in the radial direction, and thus severe contact with the rotating runner can be prevented. Leakage of floating-ring seal is much larger than that of face-contact mechanical seal, but the floating-ring seal shows a high resistance to pressure and a high reliability when used as high-pressure seal. A multi-seal system consisting of several seal rings arranged in series is employed for the high-pressure turbopumps. The floating-ring seals were developed and used in the LE-5 and LE-7.

Figure 18 shows the floating-ring seal with a seal diameter of 50 mm developed for the LO_2 turbopump of the LE-7 [22,35]. The carbon seal ring is enclosed with a retainer of the same material as the seal runner. Since the retainer contracts thermally nearly as much as the seal runner at low temperature, the seal gap hardly changes. The seal gap was 50-60μm. When the seal pressure increases, the floating ring is pressed against the secondary seal by the fluid force and its movement in the radial direction is restrained. In order to smooth the radial movement of the floating ring, on the secondary seal of the housing, the PTFE film was coated for the LO_2 seal and the MoS_2 film was coated for the turbine gas seal (to seal the low temperature GH_2). For the GH_2 leakage of the floating-ring seal used in the turbine gas seal, leakage rate calculated by the quasi-one-dimensional compressible flow equation agreed quite well with experimental value.

http://dx.doi.org/10.5772/55733

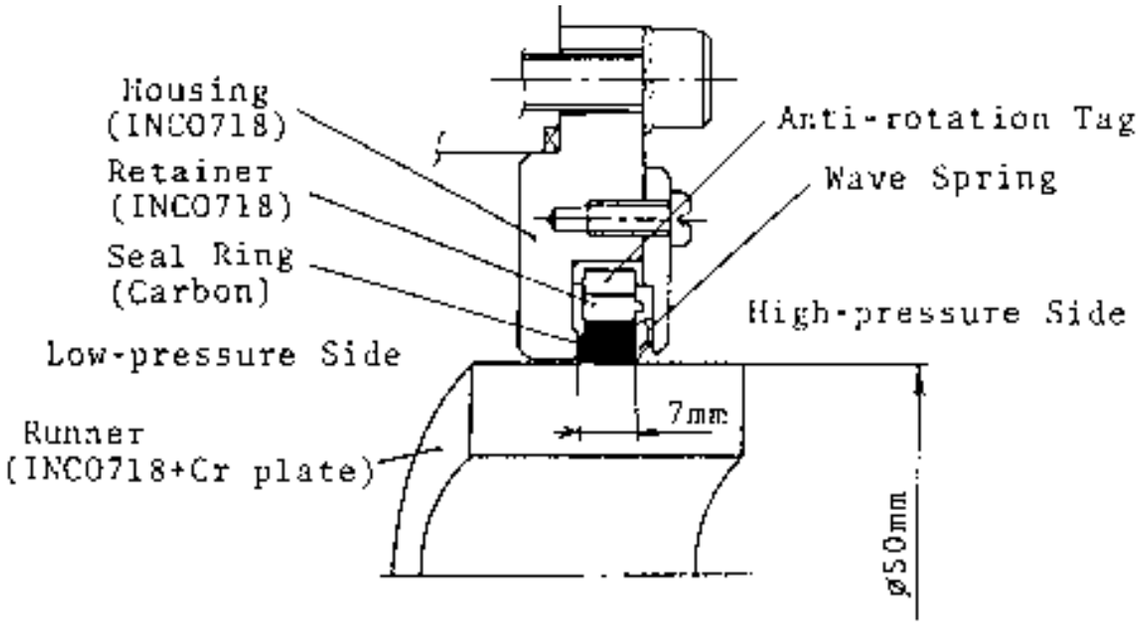

Figure 18. Floating ring seal for LO_2 turbopump of LE-7

The leakage from the floating-ring seal for the LH_2 and LO_2 seal can be calculated from the equation of the incompressible fluid flow in the rotating double cylinders when the leakage is liquid phase flow and the mass flow flux (mass flow/seal area in the flow direction) is large [29,35]. When the seal gap is narrow and the seal pressure is low, the mass flow flux of leakage is reduced, and vaporization of leakage occurred by viscous frictional heating and pressure drop changes liquid phase flow to gas-liquid phase flow (two-phase flow).

Comparison between the experimental and calculated leakage of LH_2 was evaluated by the mass flow flux of leakage for the floating-ring seal with one seal ring or two seal rings [29]. In this study, the LH_2 seal with a seal diameter of 32 mm and various seal gap of 30-86 μm was tested at rotating speeds to 50,000 rpm. It is shown that the leakage of LH_2 is less than the calculated value from incompressible fluid flow equation because the leakage is changed to be tow-phase flow. When the mass flow flux is large, most of leakage flows out in liquid phase. This means that there is not sufficient time to vaporize the leakage to be tow-phase flow within the seal gap.

A flow visualization study of floating-ring seal was conducted to identify the two-phase flow area induced by viscous frictional heating and pressure drop [36]. In order to visualize the two-phase flow in seal gap, the floating ring made of transparent hard plastic (polycarbonate) was tested in a seal fluid of LN_2. It was confirmed that the two-phase flow seemed to be homogeneous mixture of liquid and vapor flow and the two-phase flow area increases with increasing rotational speed and decreases leakage flow rate. When the two-phase flow area was fully prolonged within the seal gap, the leakage rate contrary increased with instability because the inlet flow resistance at the high-pressure side of the seal ring was reduced by two-phase flow.

5.3. Segmented seal [22, 35, 37, 38]

Contact-type segmented seal were used in the GHe purge seals and the low pressured turbine gas seals. The GHe purge seal used in the LO_2 turbopump of the LE-7 is shown in Fig. 19 [22]. Segmented seal has a carbon seal ring cut into three segments. The segmented annular seal ring is pressed on the seal runner with a coil spring and maintains high purge-pressure of GHe as a barrier gas. Wear of the carbon seal ring is reduced by using the shrouded Rayleigh step lift-pads to increase the opening force within the seal clearance. As the rubbing speed increases, the opening force in the Rayleigh step increases, so that the rubbing speed is increased by enlarging the seal diameter using a T-type runner.

Relationship between the purge pressure and the leakage rate of GHe purge seal was evaluated at a steady speed of 20,000 rpm [22]. When the purge pressure is low, the seal face is kept to be non-contact because the Rayleigh step increases the seal opening force. As the purge pressure is set to be high, the seal face condition is changed from the non-contact state to the contact state, it resulted that the dynamic leakage almost equals that of the resting state. Furthermore, for the GHe purge seal combined with the LO_2 floating-ring seal, the environmental temperature around the GHe purge seal was equal to that of LO_2 leakage, so that the carbon seal ring showed severe wear with an appearance of worn-out of the Rayleigh step.

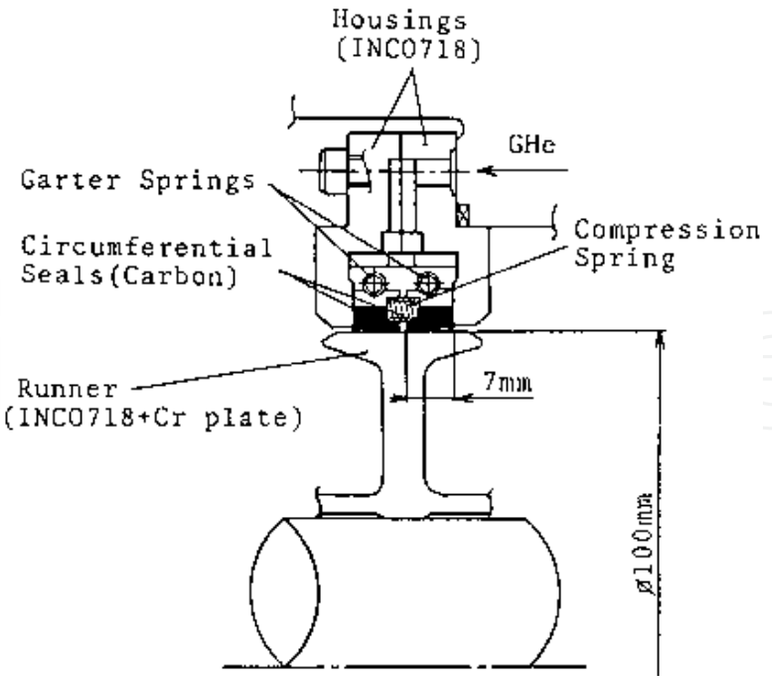

Figure 19. GHe purge seal for LO_2 turbopump of LE-7

http://dx.doi.org/10.5772/55733

Figure 20. Comparison of wear of MoS_2 coated and uncoated seal surfaces

Change of the friction and wear of the carbon pin as a function of the pin temperature was determined in the cryogenic GHe environment [23]. Friction test was conducted against the Cr-plated steel disk at a sliding speed of 12 m/s and load of 9.8 N. When the pin temperature is below the solidification temperature of CO_2 (216 K), it is noted that lubricating property of the carbon pin suddenly disappeared and friction and wear became intensive. When absorbed CO_2 gas was changed to be solid phase, lubricity of carbon was lost. This phenomenon resembles that when phase of moisture is transfer to solid phase (ice) below 273 K, lubricity decreases; be well known. From this fact, it seemed that severe wear of the GHe purge seal was generated because the environmental temperature around the seal was lower than 216 K. Spray MoS_2 coating on the carbon seal face was drastically able to prohibit progression of wear of the carbon seal ring at low temperature, as shown in Fig. 20.

After a total operating time of 29 minutes for the engine firing test, the GHe purge seal used in the LE-7 indicated that the seal surfaces coated by MoS_2 were found to be in excellent condition and wear depth of the carbon seal ring was about 7 μm. It assumes that high opening force produced by the Rayleigh step was kept by prohibit of wear of the Rayleigh step and the GHe purge seal was operated under conditions of nearly no load on the seal surfaces due to balance between the opening and closing forces.

6. Advanced bearings and shaft seals

Future space transport systems require reusable launch vehicles to reduce launch cost and to increase efficiency. The durability of reusable turbopump bearings must be greater than that

of currently available (expendable) turbopumps. For the improved high-pressure LO_2 turbopump of the SSME that reduced serious wear of the all-steel bearing, the hybrid ceramic bearing with Si_3N_4 balls was developed and accomplished the required life of 7.5 hours. In this case, to improve self-lubrication of the abrasive retainer made of glass cloth-reinforced PTFE, a new type of the retainer that had PTFE/bronze-powder insert fitted on the ball pocket was developed [7].

It is noted that, at high speeds, the hybrid ceramic bearing that consists of hard, light weight ceramic balls as well as steel rings shows a lower centrifugal force on the ceramic ball. The centrifugal force of the Si_3N_4 ball makes about 60 % lighter than that of the 440C steel ball. This leads to a reduction of bearing load and a smaller contact area with a lower spinning speed, resulting in a low level of heat generation due to ball spin. Additionally, good tribological combinations of the ceramic balls against the steel rings result in a decrease in bearing wear and in instances of seizure, even under insufficient lubricating conditions. Thus, the hybrid ceramic bearing enables higher speed operation rather than the all-steel bearing.

On the other hand, advanced rocket engines that are characterized by high performance (light weight) and high durability (long life) are required today. Ultra-high speed turbopump having a rotational speed level of 100,000 rpm needs to make engine smaller and lighter. Hybrid ceramic bearing is suitable to ultra-high speed turbopump because of lower centrifugal force. In recent years, these advanced research and development on the hybrid ceramic bearing are actively underway.

6.1. Single–guided bearing [27, 28, 39]

In order to increase the durability of self-lubricated bearing, it is apparent that sufficient cooling and restriction of the frictional heat generation in the bearing are essential. Its notification is experimentally identified by a series of studies on the turbopump bearing. In order to improve internal coolant flow through the bearing and to reduce bearing frictional torque, a new type of bearing having a single-guided retainer was developed. Figure 21 shows the 25-mm-bore bearing having a single-guided retainer with elliptical ball pockets [39]. The single-guided retainer is guided only by one side of the outer-ring bore (land) to reduce land friction and to increase the cooling ability within the bearing. However, reduce of retainer guiding is apt to generate unstable wobbling at high speed, so that the elliptical ball pockets with narrow axial clearance is needed to reduce wobbling of the retainer. For the elliptical ball pocket of the single-guided retainer, its circumferential clearance of 1.3 mm was twice as large as that of the conventional circular pocket to reduce ball-to-pocket interaction under high BSV. Furthermore, the axial clearance of 0.1 mm was narrow to stabilize wobbling of the single-guided retainer at high speeds.

Self-lubricating performance, bearing wear and transfer film of two-types of the single-guided bearing, i.e., a hybrid ceramic bearing with Si_3N_4 and all-steel bearing, was evaluated under high thrust loads at speeds up to 50,000 rpm in LH_2, LO_2 and LN_2 [27,39]. Furthermore, to evaluate the durability of the single-guided bearing for long-life bearing, the all steel bearing was tested for total operation times up to 11.7 hours at a speed of 50,000 rpm with high thrust

http://dx.doi.org/10.5772/55733

loads in LO_2 [28]. These bearings used the glass cloth-reinforced PTFE retainer which was chemically treated with HF to improve self-lubrication.

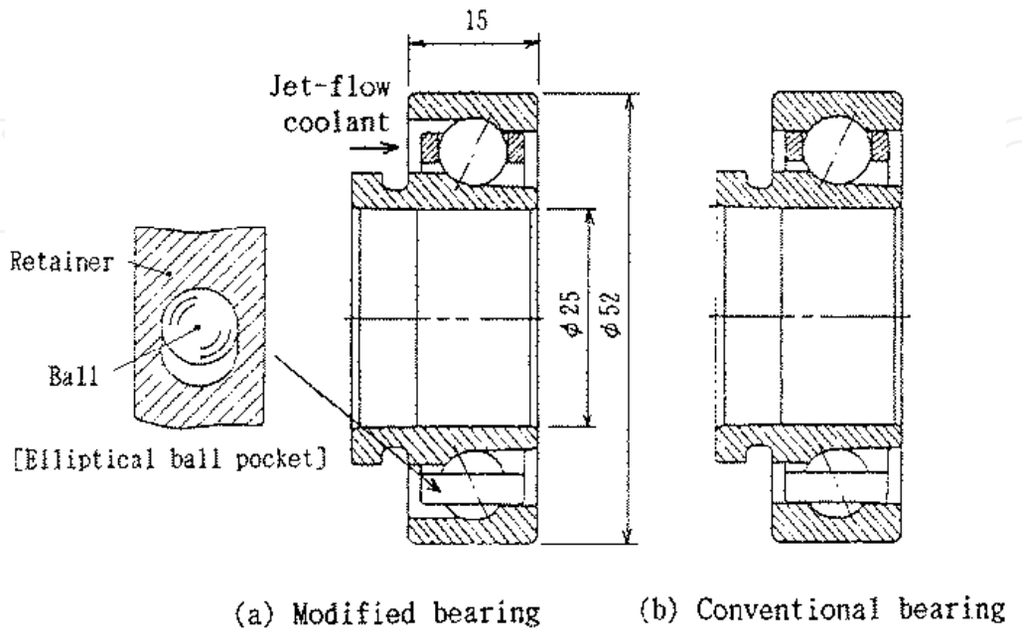

Figure 21. Advanced bearing having single-guided retainer with elliptical ball pocket

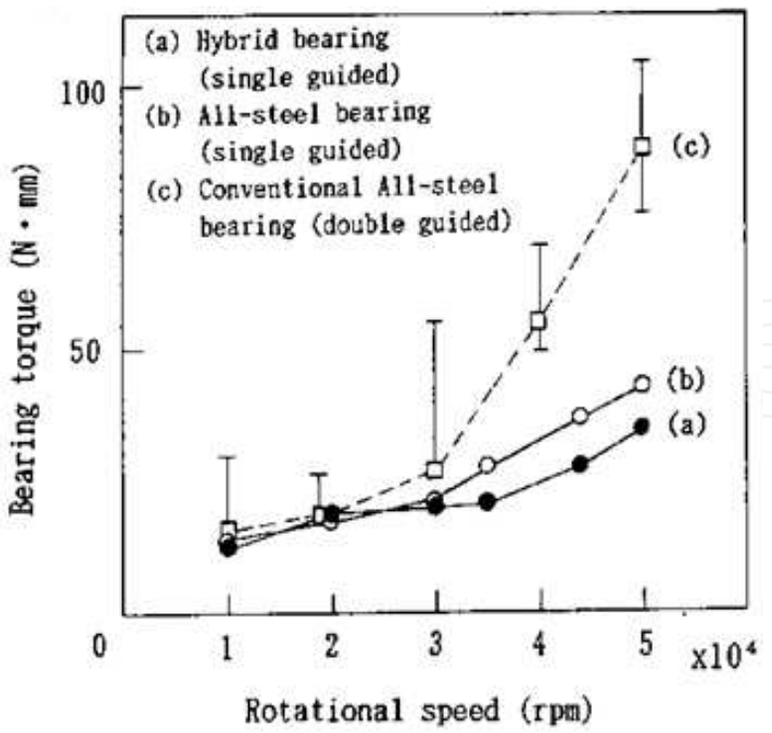

Figure 22. Bearing torque of single-guided bearings and double guided bearing to 50,000 rpm in LH_2

6.1.1. Self–lubricating performance and transfer film [27,39]

a. *In LH_2*

Figure 22 shows the bearing torque of the single-guided bearings (hybrid ceramic bearing and all-steel bearing) and the conventional double-guided bearing at speeds to 50,000 rpm in LH_2 [39]. It was observed that the bearing torque of the single-guided bearing effectively decreased to about one-half of that of the double-guided bearing. Its result identified that bearing torque induced by high-speed sliding of the outer land guide of the retainer almost accounted for an overall bearing torque generated at high speeds. In addition, the hybrid ceramic bearing showed lower bearing torque than the all-steel bearing at high speeds.

Critical load capacity of the single-guided bearing without a significant rise of the bearing torque and bearing temperature was evaluated. For the single-guided hybrid ceramic bearing tested in LH_2, the critical thrust load was 1,960 N (*Smax* of inner race, 2.7 GPa) at 50,000 rpm and was two times higher than that of the double-guided all-steel bearing. Furthermore, even when bearing torque increased with a rise of bearing temperature, the hybrid ceramic bearing was able to sustain a thrust load of 2,840 N (*Smax*, 3.2 GPa) at 50,000 rpm without seizure in LH_2. High critical load capacity of the single-guided hybrid ceramic bearing was demonstrated [39].

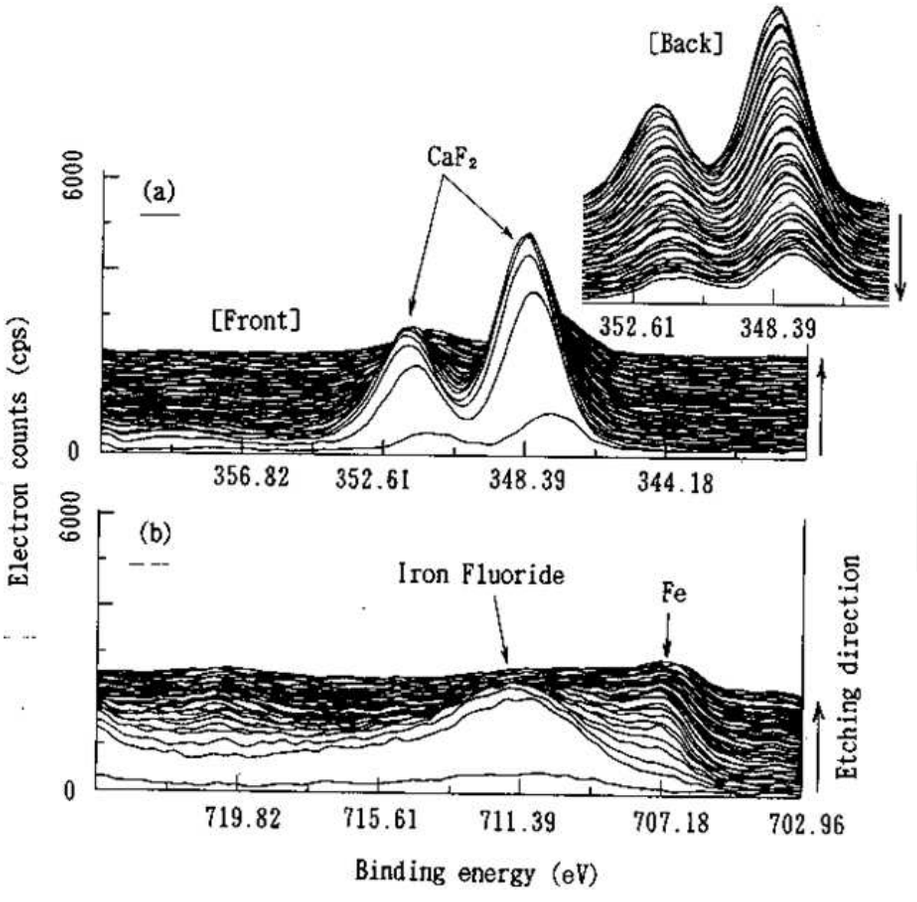

Figure 23. XPS depth analysis of Si_3N_4 ball of hybrid ceramic bearing tested in LH_2

Figure 23 shows the XPS depth analysis of a Si_3N_4 ball taken from the hybrid ceramic bearing tested in LH_2 [27]. Its etching depth was 120 nm (SiO_2 rate). It was found that a considerably thick transfer film consisting of CaF_2/FeF_2 was formed on the ceramic balls. CaF_2 and FeF_2 seemed to be tribo-chemically formed by the reducing power of LH_2. The considerably thick transfer film of CaF_2 and FeF_2 led to exhibit high load capacity. For the all-steel bearing tested in LH_2, a thick CaF_2 film was formed beneath an extremely thin PTFE overlay, but its thickness of CaF_2 transfer film was thinner than that of the hybrid ceramic bearing.

b. *In LO_2*

In LO_2, the hybrid ceramic bearing exhibited poor self-lubricating performance even at a low speed of 10,000 rpm. To the contrary, the all-steel bearing indicated excellent load capacity accompanied by a stable bearing and enabled to sustain a thrust load of 2,650 N (*Smax*, 2.7 GPa) at a speed of 50,000 rpm without seizure in LO_2 [39].

For the hybrid ceramic bearing, an extremely thin, weakly adhesive PTFE film was formed on ceramic balls and resulted in a poor load capacity of the bearing. For the all-steel bearing, the intense formation of a Cr_2O_3 film was beneath an extremely thin PTFE film. It is noted that the tribo-chemical formation of Cr_2O_3 film due to high oxidation power of LO_2 could exhibit high resistance to metal-to-metal adhesion leading to seizure [27].

c. *In LN_2*

The hybrid ceramic bearing exhibited better load capacity than that of the all-steel bearing in LN_2. The hybrid ceramic bearing enabled to sustain a thrust load of 2,700 N (*Smax*, 3.1 GPa) at a speed of 50,000 rpm without seizure. To the contrary, the all-steel bearing showed unstable change of bearing torque and seized at a relatively light-thrust load of 1,470 N (*Smax*, 2.2 GPa) at a speed of 50,000 rpm [39].

For the hybrid ceramic bearing, the thick transfer film consisting of FeF_2/iron oxide formed on the ceramic balls. To the contrary, the seized all-steel bearing was lubricated by only thin PTFE transfer film, without the tribo-chemical formation of $CaF_2/FeF_2/Cr_2O_3$ films because of its inert environment of LN_2. This fact was determined by that the all-steel bearing once tested in LH_2 or LO_2, whose bearing formed the $CaF_2/FeF_2/Cr_2O_3$ films, showed stable change of the bearing torque without seizure even under high thrust loads above 1,470 N in LN_2 [27].

6.1.2. Long–life bearing [28]

The single-guided all steel bearing was tested for a total operation time to 11.7 hours at a speed of 50,000 rpm with high thrust loads to 2,400 N in LO_2. During long-run test, one-hour operation at a speed of 50,000 rpm was repeated nine times. The test bearing was effectively cooled by the jet-cooling with using nozzles. During the long-run test, the bearing exhibited stable variation of the bearing torque in a range of 93-95 N-mm [28]. The bearing exhibited excellent self-lubrication performance that there was no abnormal change of the bearing torque and bearing temperature.

From the examination of the bearing tested for the long-run test in LO_2, it was observed that sound surface conditions with hardly any wear were determined. The XPS depth

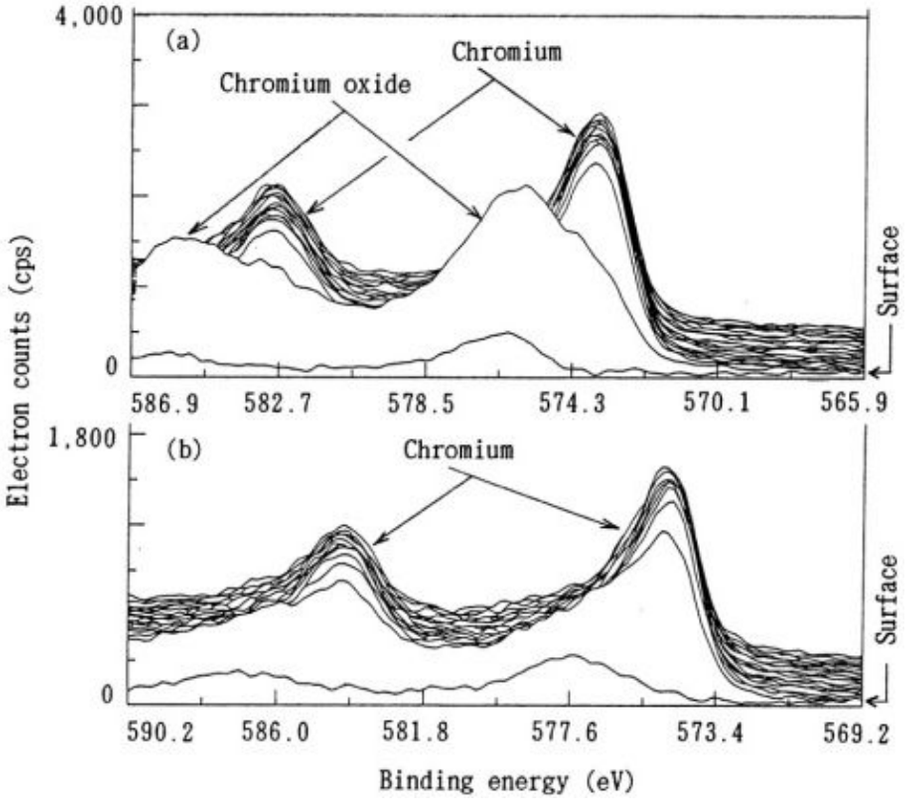

Figure 24. XPS depth analysis of SUS440C ball tested for long run in LO_2 and new ball

analysis of a ball taken from the tested bearing is shown in Fig. 24 [28]. Its etching depth was 30 nm (SiO_2 rate). It is noted that the intense formation of a Cr_2O_3 film was detected and its thickness was thicker than that of the native Cr_2O_3 film on the new ball. Under sufficient cooling conditions in LO_2, the thick Cr_2O_3 film formed by tribo-chemical reaction could provide an extremely high resistance to metal-to-metal adhesion beneath an extremely thin CaF_2 film. To the contrary, under poor cooling conditions in LO_2, the intense formation of oxide film (Fe_2O_3) was mainly produced and led to large mild wear, as discussed in the LO_2 turbopump bearing. Furthermore, the formation of Fe_2O_3 might reduce adhesion of PTFE transfer film, resulting in less lubricant within the bearing. The results indicated that thick formation of a Cr_2O_3 film due to tribo-chemical reaction in LO_2 is important to reduce the bearing wear. Its effect needs sufficient cooling with jet within the bearing components to eliminate the formation of Fe_2O_3 [28].

6.2. Fluorine–passivated bearing [28]

It is experimentally found that the FeF_2 film formed by a tribo-chemical reaction between the F of PTFE and Fe of 440C steel was facilitated by the high reduction power of LH_2 and enhanced to reduce the bearing wear in LH_2. This may suggest that the FeF_2 film has a good solid-lubricant performance to improve the tribological performance of the bearing. Effect of the coated FeF_2 film on the self-lubrication and durability of the all-steel bearing was evaluated. An FeF_2 film was chemically formed by means of a passivating surface treatment of fluorida-

http://dx.doi.org/10.5772/55733

tion in hot pure F_2 gas. The fluorine-passivated bearings coated with FeF_2 film was tested by long run for 11.7 hours at a speed of 50,000 rpm under high thrust loads in LH_2, LO_2 and LN_2. The fluorine-passivated bearings showed excellent self-lubrication in both LH_2 and LN_2 [28].

In a reduce environment of LH_2, even under poor cooling conditions controlled by reducing of the coolant flow, the fluorine-passivated bearing exhibited superior durability for a total test time to 4.4 hours, as compared with signs of seizure for the untreated bearing. The XPS analysis of the transfer film indicated that the fluorine-passivated bearing was tribo-chemically lubricated by a thick CaF_2 film overlaid on a thick FeF_2/Cr_2O_3 films.

In an inert environment of LN_2, the fluorine-passivated bearing showed excellent self-lubrication and wear conditions for the long-run test up to 11.7 hours at a speed of 50,000 rpm. Stable change of the bearing torque (75-80 N-mm) was shown for the passivated bearing during the long-run test in LN_2 [28]. The bearing test was repeated seven times at a speed of 50,000 rpm and a thrust load of 2,600 N in LN_2. From the examination of the fluorine-passivated bearing tested in LN_2, sound surface conditions with hardly any wear were determined. It was found that a thick CaF_2 film was tribo-chemically formed on thick FeF_2/Cr_2O_3 films of the bearing. On the other hand, the untreated bearing was seized at a low thrust load of 1,470 N due to less tribo-chemical reaction in LN_2, as mentioned before. In such inert environment in LN_2, there was less formation of $CaF_2/FeF_2/Cr_2O_3$ films, so that poor self-lubrication and load capacity of the bearing were shown.

To the contrary, in an oxide environment of LO_2, the fluorine-passivated bearing indicated a higher bearing torque with greater unstable change than that of the untreated bearing [28]. The bearing tests were repeated seven times of the bearing test at a speed of 50,000 rpm and a thrust load of 2,450 N in LO_2. Its total test time was 11.7 hours. During long-run test, high bearing torque continued to vary erratically with the variation in a range of 75-120 N-mm. The fluorine-passivated bearing tested in LO_2 showed somewhat high wear. To the contrary, the untreated bearing demonstrated excellent self-lubrication with hardly any wear during the long-run test as mentioned before. It was clearly showed that the FeF_2 film in LO_2 made a typical reduction in self-lubrication.

Inspection of the fluorine-passivated bearing tested in LO_2 indicated that the initial coated film of FeF_2 was worm away. Its result also indicated that oxide power of LO_2 restricted the tribo-chemical formation of FeF_2 film. Such reduction in self-lubrication possibly resulted from that the coated FeF_2 film restricted the tribo-chemical formation of Cr_2O_3 film in LO_2, resulting in an increase of metal-to-metal adhesion. These results indicated that excellent lubrication depended on the tribo-chemical formation of CaF_2/FeF_2 films in LH_2 or Cr_2O_3 film in LO_2, respectively. In order to obtain high self-lubrication and durability of the bearing, it is noted that tribo-chemical reaction is necessary at the frictional interfaces within the bearing [4].

6.3. Ultra–high–speed hybrid ceramic bearing [8,40]

Based on previous bearing tests at high speeds up to 50,000 rpm, the hybrid ceramic bearing (25-mm bore) was tested at ultra-high-speeds up to 120,000 rpm, and results were compared with the all-steel bearing in LH_2. At a ultra-high speed of 120,000 rpm, the inner-race growth

of 34μm due to centrifugal force results in a reduction of the radial clearance within the bearing. Table 4 summarizes comparison of the bearing load and speed conditions for the hybrid ceramic bearing and all-steel bearing at a speed of 120,000 rpm with a thrust load of 980 N [8]. At 120,000 rpm, the initial radial clearance of 77 μm was decreased to 43μm. For the hybrid ceramic bearing, the maximum contact stress *Smax* at the inner race is apt to increase rather than that of the all-steel bearing due to a high elastic modulus. However, the maximum spinning velocity *Vmax* is reduced and resulted in a lower *SVmax* value that leads to a reduction of the bearing temperature and spin wear. The maximum contact stress at the outer race becomes higher due to centrifugal force. For sliding conditions of the retainer, the sliding velocity at the outer land and ball pocket reaches to a high level of 110 m/s and the frictional heat generation of the retainer is to be severe. For the cooling system to remove the bearing heat generation at 120,000 rpm, effective jet cooling with nozzles needs to obtain sufficient coolant flow within the bearing. The nozzles were directed to cool the single outer land-guiding side of the retainer where high frictional heat is generated.

Parameters	Hybrid ceramic bearing	All-steel bearing
Bearing		
Rotational speed [rpm]	120,000	
Thrust load [N]	980	
Initial contact angle [deg.]	20	
Initial radial clearance [μm]	77	
Operational radial clearance [μm]	43	
Maximum contact stress at inner/outer races (*Smax*) [GPa]	2.31 / 2.14	2.00 / 2.35
Maximum spinning velocity at inner race (*Vmax*) [m/s]	5.8	7.5
Centrifugal force on ball [N]	454	1,120
Retainer		
Sliding velocity at outer land [m/s]	108	
Sliding velocity at ball pocket [m/s]	116	

Table 4. Bearing load and speed conditions for hybrid ceramic and all-steel bearings at 120,000 rpm with 980 N (25-mm bore)

Figure 25 shows the change of the bearing temperature at a steady speed of 120,000 rpm with a thrust load of 2,160 N [8]. The hybrid ceramic bearing showed excellent performance with a stable condition of the bearing temperature, compared to the seized all-steel bearing showing an irregular change of high bearing temperature. When the thrust load was increased to 3,140 N, the hybrid bearing showed slight damage with a spiky rise of the bearing temperature. It was found that the critical load capacity *Smax* without seizure at a speed of 120,000 rpm was reached to 3.0 GPa (at a thrust load of 2,160 N) for the hybrid ceramic bearing and 2.0 GPa (980 N) for the all-steel bearing, respectively.

http://dx.doi.org/10.5772/55733

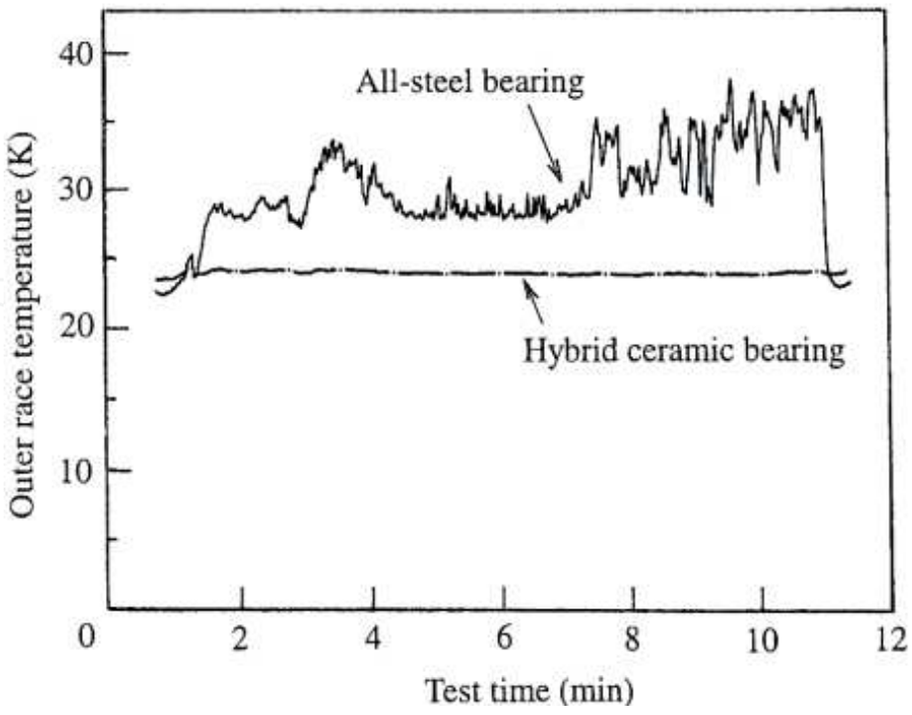

Figure 25. Change of bearing temperature of hybrid ceramic and all-steel bearings at 120,000 rpm with 2,160 N

The power loss around the bearing was estimated based on the heat absorbed by the cooling flow [8]. Figure 26 shows the power loss of the hybrid ceramic and all-steel bearings as a function of rotational speed up to 120,000 rpm in LH_2 under different cooling conditions at a thrust load of 980 N. It was found that the power loss of the bearing significantly increased above 80,000 rpm with increasing cooling flow rate. At 120,000 rpm, the power loss of the bearing that contained the viscous power loss of 2.2 kW at the shaft side was estimated. The power loss was 6.0 kW for the hybrid ceramic bearing and 6.4 kW for the all-steel bearing, respectively. There was not typical difference of the power loss of the bearing because viscous power loss within the bearing almost accounted for an overall power loss generated at ultra-high speeds. It seems that the power loss around the bearing was mainly induced by viscous drag and churning of the cooling flow passing through the bearing.

The components of the hybrid ceramic bearing were in excellent condition with regard to wear at a speed of 120,000 rpm with a thrust load of 3,140 N in LH_2 [40]. On the contrary, the seized all-steel bearing exhibited severe adhesive wear. It was found that the ceramic balls formed superficial micro-cracks on the contact track. Superficial micro-cracks visually extended in a mesh-like pattern on the Si_3N_4 ball tested. It was shown that network of hair crack was propagated along wide-ditch crack. A marked feature of these superficial micro-cracks was that they were very shallow to about 3 μm at maximum and did not extend deeply into the ball. From detailed observation with a scanning electron microscope (SEM), such wide-ditch cracks seemed to be formed by removal of fragments fractured due to contact stress repeated by the rolling balls as shown in Fig. 27. Thus, when the Si_3N_4 balls had lower mechanical strength and fracture toughness, it was clear that wide-ditch cracks were apt to be formed.

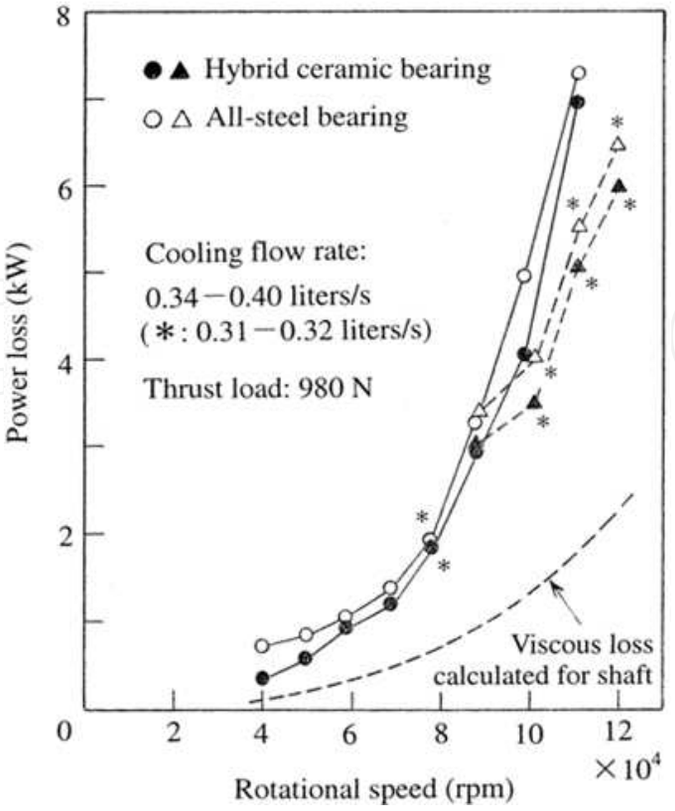

Figure 26. Power loss of hybrid ceramic and all-steel bearings as a function of rotational speed up to 120,000 rpm in LH_2

An advanced study was conducted to select a tough Si_3N_4 ball capable of restraining crack propagation as well as to evaluate the efficient bearing cooling with nozzles. A Si_3N_4 ball having higher thermal-shock resistance, as well as higher fracture toughness, was found to reduce the propagation of superficial micro-cracks, resulting in a decrease of ball wear. Furthermore, it was observed that the cooling ability of the LH_2 jet-flow aimed at the retainer was superior to that aimed at the inner raceway, further reducing the propagation of thermal micro-cracks on the Si_3N_4 balls. This result also indicated that micro-cracks on the balls were possibly generated at the trace contacting the outer raceway due to a higher centrifugal force under insufficient cooling conditions. Furthermore, under the same cooling rate, the four nozzles achieved a higher cooling ability than the two nozzles with increasing jet speed above 208 m/s. The jet-speed of nozzles reached to the twice of the sliding speed of 108 m/s at the retainer outer-land [40].

In order to prevent the propagation of superficial thermal micro-cracks on the balls, the outer race contact stress was reduced by decreasing the outer race curvature to a limited value of 0.51. Furthermore, sufficient cooling at the outer raceway was gained by a proper clearance of the outer land of the retainer. Decreasing the maximum outer-race stress to 2.0 GPa (thrust load, 1,960 N) in conjunction with sufficient cooling through a narrow outer land clearance could prevent the propagation of superficial micro-cracks even under insufficient cooling conditions [40].

http://dx.doi.org/10.5772/55733

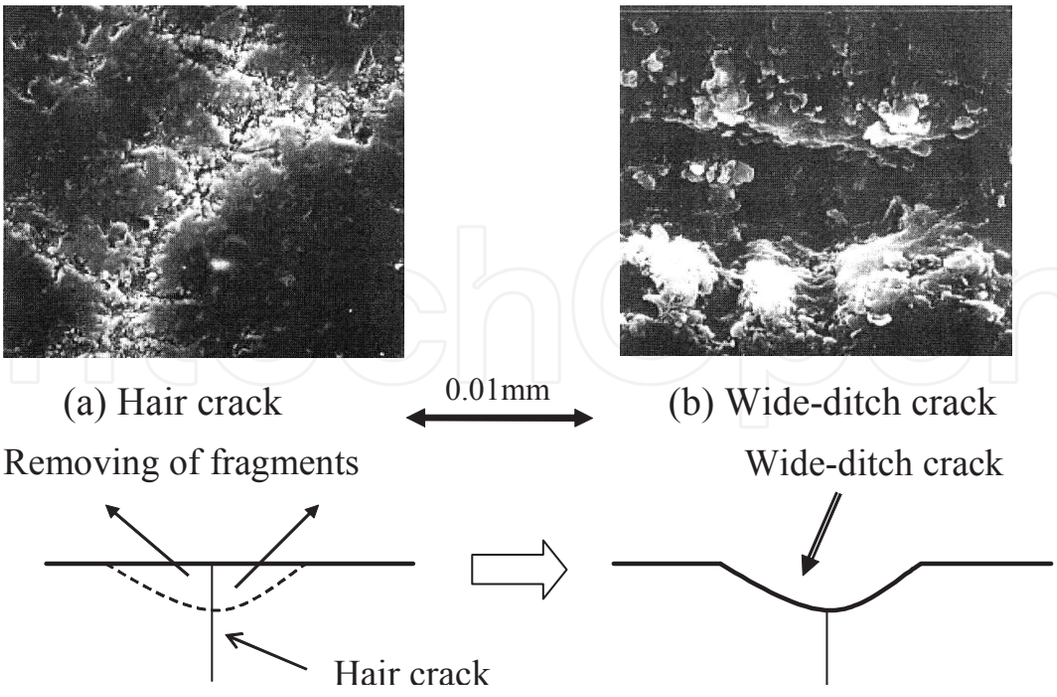

Figure 27. Process model of wide-ditch crack formation on Si_3N_4 ball

6.4. Ultra–high–speed two–phase seal [8]

The floating-ring seal due to noncontact-type is suitable for high-pressure turbopumps; however, conventional seals using carbon seal-rings were weak under high speed and high pressure conditions. Since metal seal-rings have higher mechanical strength and durability, advanced floating-ring seal (with one-seal and two-seal rings) that used Ag-plated metal seal-rings with a seal diameter of 30 mm [8]. This metal seal was studied at ultra-high speeds up to 120,000 rpm in LH_2. Calculated runner growth due to centrifugal force at 120,000 rpm was 29μm, so that the initial seal clearance (gap) was decreased as the rotational speed increased. The test seal had an Ag-plated seal ring made of Inconel 718 that was the same material used for the runner. The runner was coated with a Cr_2O_3 plasma spray, and this coating exhibited excellent friction and wear without adhesion to Ag in LN_2. In order to obtain smooth radial movement of the seal ring, the static seal surface of the housing was coated with a sprayed MoS_2 film.

Figure 28 shows the seal performance of the one-ring seal *vs.* the two-ring seal up to a speed of 100,000 rpm in LH_2 [8]. These seals had a straight bore with a seal gap of 110-120 μm. Figure 29 also shows the phase change models of leakage flow within the seal gap [4]. Seal performance depended on the two-phase flow (gas/liquid phase) of leakage, because the vaporization of leakage was generated by the viscous friction heat and by the seal pressure drop. At lower speeds, the leakage of the one-ring seal was relatively greater than that of the two-ring seal; however, with increasing speed, the leakage of the one-ring seal was drastically decreased and approached the same level of the two-ring seal due to enlargement of the two-phase flow.

For the two-ring seal, the two-phase flow was fully enlarged within the secondary seal ring that was at the downstream of the primary seal ring. Seal leakage was reduced within limits; however, the hydrodynamic force of the liquid phase flow that sustained the seal ring was lost and resulted in seal-ring seizure at a relatively lower speed of 98,700 rpm. Also, shaft vibration for the two-ring seal was likely produced by wobbling of the seal ring under severe rubbing conditions and abruptly increased at speeds of more than 92,000 rpm before resulting in seal-ring seizure at a speed of 98,700 rpm. Furthermore, in the two-ring seal with a seal gap of 70-80 μm, the primary seal-ring seized a speed of 108,600 rpm, because the hydrostatic force decreased due to a low differential pressure.

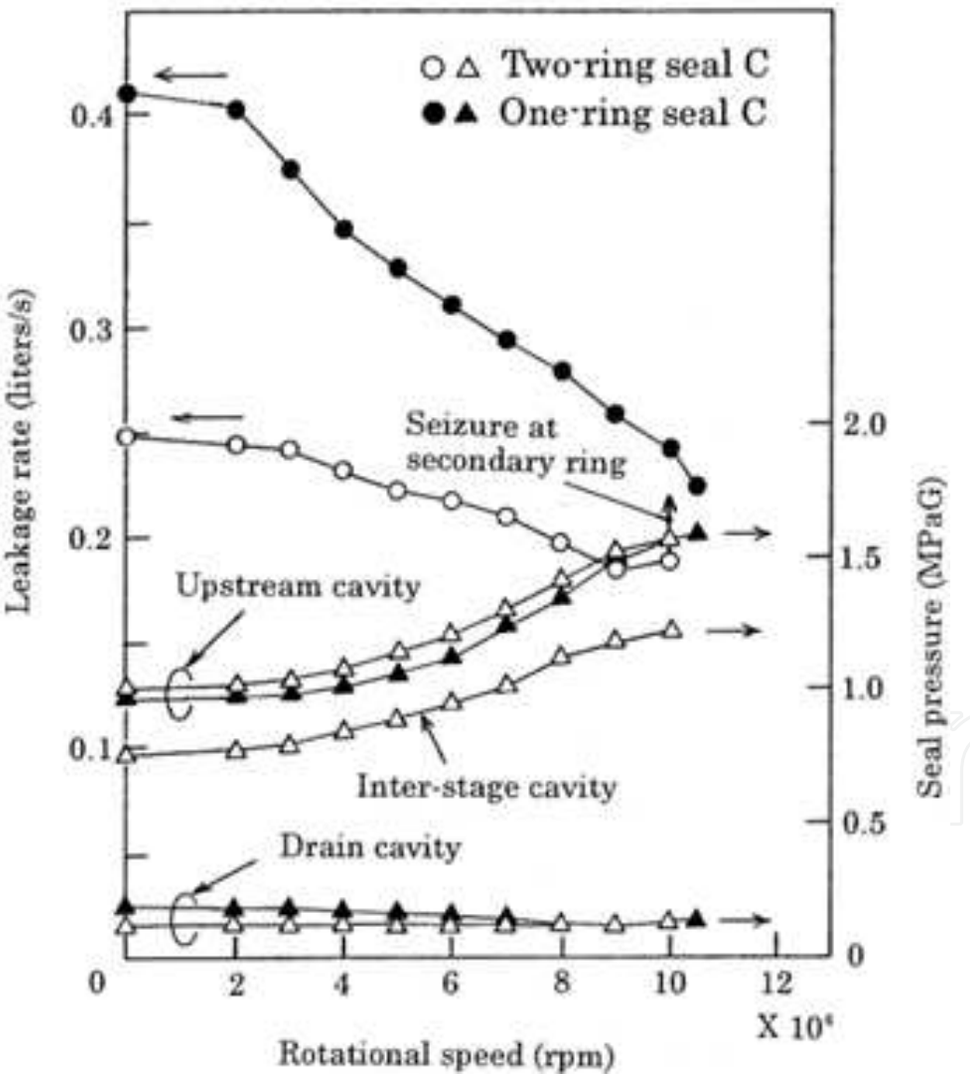

Figure 28. Seal performance of one-ring seal *vs.* two-ring seal up to 100,000 rpm

http://dx.doi.org/10.5772/55733

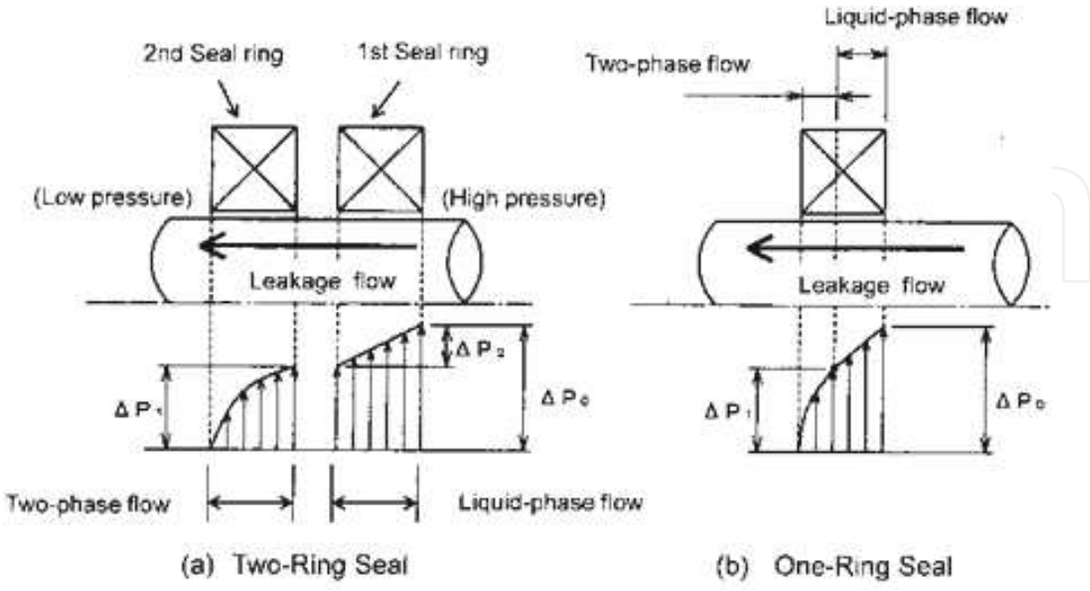

Figure 29. Phase change models of leakage flow within seal gap at ultra-high speed

In contrast, the one-ring seal successfully functioned with no abnormal signs of seizure during tests, because the liquid-phase flow remained within a seal clearance even though the two-phase flow increased. As a result, the hydrodynamic force in the liquid-phase flow as well as the hydrostatic force due to high differential pressure possibly helped to prevent seal-ring seizure. At a steady speed of 120,000 rpm, the one-ring seal exhibited a stable leakage in a range of 0.21-0.24 liters/s that is similar to leakage in the two-ring seal as shown in Fig. 28. Thus, the one-ring seal was superior to the two-ring seal, preventing seal-ring seizure due to an increase of two-phase flow within the sealing clearance.

7. Concluding remarks

For built-up of safe space transport system to achieve high reliability, cryogenic high-speed bearing and shaft seal used in the rocket turbopumps are reviewed historically. These tribo-components have specific lubrication, materials and design requirements in pumping cryogenic liquid propellants in rocket engines. Nowadays, as earth scale issues of energy conservation and environment preservation, a breakaway from the conventional fossil-fuel society becomes a big problem. Clean hydrogen energy is attractive due to its energy efficiency and its smaller impact on the environment, and it is expected to be a key technology in the 21st century. It is proposed that, to build hydrogen infrastructure for LH_2 storage and distribution, development of an industrial tribo-system with long durability and high reliability is essential and advances by supporting of cryogenic tribology studied for LH_2 rocket system.

Acknowledgements

This paper is based on previous cryogenic tribology studies carried out by Japan Aerospace Exploration Agency (JAXA) at Kakuda Space Center. These studies were also supported by IHI Corporation for turbopumps, by NTN corporation for bearings and by Eagle Industry Co., LTD. for shaft seals, respectively. The author is indebted to researchers engaged for their valuable support, to organizations for their enthusiastic cooperation. At last, the author has to thank late Prof. Miyakawa, Y. of Hhosei University, as a pioneer in space tribology in Japan, for his guidance to cryogenic tribology with profound appreciation.

Author details

Masataka Nosaka and Takahisa Kato

Department of Mechanical Engineering, University of Tokyo, Tokyo, Japan

References

[1] Dieter K H & David H H. Modern Engineering for Design of Liquid-Propellant Rocket Engines, *Progress in Astronautics and Aeronautics, Vol. 147*, AIAA, (1992), 155-218.

[2] Liquid Rocket Engine Turbopump Bearing, NASA SP-8048, 1971.

[3] Liquid Rocket Engine Turbopump Rotating- Shaft Seals, NASA SP-8121, 1978.

[4] Nosaka, M. Cryogenic Tribology of High-Speed Bearings and Shaft Seals in Liquid Hydrogen, *Tribology Online*, 6, 2, (2011), 133-141.

[5] Nosaka M, Takada S & Yoshida M. Research and Development of Cryogenic Tribology of Turbopumps for Rocket Engines, *J. of Aeronautical and Space Science Japan*, 58, 681, (2010), 303-313, in Japanese.

[6] Hale J R & Klatt F T. SSME Improvement for Routine Shuttle Operations, AIAA-85-1163, (1985).

[7] Gibson H. Lubriction of Space Shuttle Main Engine Turbopump Bearings, *Lubr. Eng.* 57, 8, (2001), 10-12.

[8] Nosaka M, Takada S, Kikuchi M, Sudo T & Yoshida M. Ultra-High-Speed Performance of Ball Bearings and Annular Seals in Liquid Hydrogen at Up to 3 Million DN (120,000 rpm), *Trib. Trans.*, 47, (2004), 43-53.

[9] Ohta T, Kimoto K, Kawai T, Motomura T, Russ M & Paulus T. Design, Fabrication and Test of the RL60 Fuel Turbopump, AIAA-2003-5073, (2003).

[10] Collongeat L, Edeline E, Frocot M & Dehouve J. Development status of high DN LH2 bearings in Snecma, AIAA-2005-3950, (2005).

[11] Rachuk V & Titkov N. The First Russian LOX-LH_2 Expander Cycle LRV: RD0146, AIAA-2006-4904, (2006).

[12] Nosaka M, Oike M, Kamijo K, Kikuchi M & Katsuta H. Experimental Study on Lubricating Performance of Self-Lubricating Ball Bearings for Liquid Hydrogen Turbopump, *Lubr. Eng.*, 44, 1, (1988), 30-44 .

[13] Nosaka M, Oike M, Kikuchi M, Kamijo K & Tajiri M. Tribo-Characteristics of Self-Lubricating Ball Bearings for the LE-7 Liquid Hydrogen Rocket-Turbopump, *Trib. Trans.*, 36, 3, (1993), 432-442.

[14] Nosaka M, Oike M, Kikuchi M, Nagao R & Mayumi T. Evaluation of Durability for Cryogenic High-Speed Ball Bearings for LE-7 Rocket Turbopumps, *Lubr. Eng.*, 52, 3, (1996), 221-233.

[15] Nosaka M, Oike M, Kikuchi M, Kamijo K & Tajiri M. Self-Lubricating Performance and Durability of Ball Bearings for the LE-7 Liquid Oxygen Rocket-Turbopump, *Lubr. Eng.*, 49, 9, (1993), 677-688.

[16] Nosaka M, Oike M & Kikuchi M. Tribology at Low and High Temperatures, Lubrication in Rocket-Turbopumps, *J. of Japan Society of Lubrication Engineers*, 33, 2, (1988), 90-96, in Japanese.

[17] Nosaka M. Self-Lubricating Performance of High-Speed Ball Bearing for Liquid Hydrogen (1), Design Problems, *J. of Japan Society of Lubrication Engineers*, 32, 10, (1987), 689-695, in Japanese.

[18] Nosaka M. Self-Lubricating Performance of High-Speed Ball Bearing for Liquid Hydrogen (2), Self-Lubricating Performance Improvements. *J. of Japan Society of Lubrication Engineers*, 32, 12, (1987), 833-838, in Japanese.

[19] Winn L W, Eusepi M W & Smalley A J. Small, High-Speed Bearing Technology for Cryogenic Turbo-Pumps, NASA CR-134615, 1974.

[20] Edmond E B & William J A. Advanced Bearing Technology, NASA SP-38, 1965.

[21] Nosaka M & Oike M. Rotating-Shaft Seals in Rocket-Turbopumps, *J. of Japanese Society of Tribologists*, 35, 4, (1990), 233-238, in Japanese.

[22] Oike M, Nosaka M, Watanabe Y, Kikuchi M & Kamijo K. Experimental Study on High-Pressure Gas Seals for a Liquid Oxygen Turbopump, *STLE Trans.*, 31, 1, (1988), 91-97.

[23] Nosaka M, Oike M & Kikuchi M. Cryogenic Tribology of Turbopumps for Rockets, *Cryogenic Engineering*, 31, 10, (1996), 500-511, in Japanese.

[24] Nosaka M. Tribological Burn-Out of Wear, *J. of Japanese Society of Tribologists*, 36, 9, (1991), 689-691, in Japanese.

[25] Nosaka M. Tribology in Low Temperature Environment, *J. of Japanese Society of Tribologists*, 52, 11, (2007), 759-764, in Japanese.

[26] Nosaka M, Takada S, Yoshida M, Kikuchi M, Sudo T & Nakamura S. Effect of Tilted Misalignment of Tribo-Characteristics of High-Speed Ball Bearings in Liquid Hydrogen, *Tribology Online*, 5, 2, (2010), 71-79.

[27] Nosaka M, Kikuchi M, Oike M & Kawai N. Tribo-Characteristics of Cryogenic Hybrid Ceramic Ball Bearings for Rocket Turbopumps: Bearing Wear and Transfer Film, *Trib. Trans.*, 42, 1, (1999), 106-115.

[28] Nosaka M, Kikuchi M, Kawai N & Kikuyama H. Effect of Iron Fluoride Layer on Durability of Cryogenic High-Speed Ball Bearings for Rocket Turbopumps, *Trib. Trans.*, 43, 2, (2000), 163-174.

[29] Suzuki M, Nosaka M, Kamijo K & Kikuchi M. Research and Development of a Rotating- Shaft Seals for a Liquid Hydrogen Turbopump, *Lubr. Eng.*, 42, 3, (1986), 162-169.

[30] Nosaka M, Miyakawa Y, Kamijo K, Suzuki M & Kikuchi M. Study on Sealing Characteristics of High Speed, Contacting Mechanical Seals for Liquid Hydrogen (Part 1), Development of Mechanical Seal for Liquid Hydrogen Turbopump, *J. of Japan Society of Lubrication Engineers*, 29, 1, (1984), 35-42, in Japanese.

[31] Nosaka M, Kamijo K, Suzuki M, Kikuchi M & Miyakawa Y. Study on Sealing Characteristics of High Speed, Contacting Mechanical Seals for Liquid Hydrogen (Part 2), Starting Torque and Static Sealing Performance, *J. of Japan Society of Lubrication Engineers*, 29, 1, (1984), 43-49, in Japanese.

[32] Nosaka M, Kamijo K, Suzuki M, Kikuchi M & Miyakawa Y. Study on Sealing Characteristics of High Speed, Contacting Mechanical Seals for Liquid Hydrogen (Part 3), Friction Power Loss and Dynamic Sealing Performance, *J. of Japan Society of Lubrication Engineers*, 29, 2, (1984), 113-120, in Japanese.

[33] Nosaka M, Kamijo K, Suzuki M, Kikuchi M & Miyakawa Y. Study on Sealing Characteristics of High Speed, Contacting Mechanical Seals for Liquid Hydrogen (Part 4), Characteristics of Running Process and Wear of Rubbing Seal Faces, *J. of Japan Society of Lubrication Engineers*, 29, 2, (1984), 121-128, in Japanese.

[34] Nosaka M, Kamijo K, Suzuki M, Kikuchi M & Miyakawa Y. Study on Sealing Characteristics of High Speed, Contacting Mechanical Seals for Liquid Hydrogen (Part 5), The Formation of Thermal Crack and Wear in Chromium Plate on Rotating Ring, *J. of Japan Society of Lubrication Engineers*, 29, 3, (1984), 187-194, in Japanese.

[35] Oike M, Nosaka M, Kikuchi M & Watanabe Y. Performance of A Shaft Seal System for The LE-7 Rocket Engine Oxidizer Turbopump, *Proc. of The 18th Inter. Symposium on Space Tech. and Sci., Kagoshima*, (1992), 143-154.

[36] Oike M, Nosaka M, Kikuchi M & Hasegawa S. Two-Phase Flow in Floating-Ring Seals for Cryogenic Turbopumps, *Tribo. Trans.*, 42, 2, (1999), 273-281.

[37] Oike M, Nosaka M, Kikuchi M & Watanabe Y. Performance of a Segmented Circumferential Seal for a Liquid Oxygen Turbopump (Part 1), Sealing Performance, *J. of Japanese Society of Tribologists*, 37, 4, (1992), 339-346, in Japanese.

[38] Oike M, Nosaka M, Kikuchi M & Watanabe Y. Performance of a Segmented Circumferential Seal for a Liquid Oxygen Turbopump (Part 2), Durability, *J. of Japanese Society of Tribologists*, 37, 5, (1992), 389-396, in Japanese.

[39] Nosaka M, Kikuchi M, Oike M & Kawai N. Tribo-Characteristics of Cryogenic Hybrid Ceramic Ball Bearings for Rocket Turbopumps: Self-Lubricating Performance, *Trib. Trans.*, 40, 1, (1997), 21-30.

[40] Nosaka M, Takada S, Yoshida M, Kikuchi M, Sudo T & Nakamura S. Improvement of Durability of Hybrid Ceramic Ball Bearings in Liquid Hydrogen at 3 Million DN (120,000 rpm), *Tribology Online*, 5, 1, (2010), 60-70.

IntechOpen